Cost-effective PROton Exchange MEmbrane WaTer Electrolyser for Efficient and Sustainable Power-to-H2 Technology

Grant No. 862253

***Start date**: 01.04.2020 – **Duration**: 36 months*
***Project Coordinator**: Daniel García-Sánchez - DLR*

D1.1: 1st report on development of electro-catalysts: Initial performance and risk assessment

WP1 Catalyst Development

WP Leader: *CENmat*
Deliverable Responsible: *CENmat*
Deliverable Author(s): Sambal S Ambu, Seyed Schwan Hosseiny, Miriam Goll (CENmat)
Antonino S. Aricò, Stefania Siracusano, Fabiola Pantò (CNR-ITAE)
Jorge Torrero, María Retuerto, Sergio Rojas (CSIC)

Status: F
(D: Draft, FD: Final Draft, F: Final)
Dissemination level: PU
(PU: Public, CO: Confidential,
only for Consortium members (including the Commission Services))

This project has received funding from the European Union's Horizon 2020 research and innovation programme under grant agreement No 862253

This project has received funding from the European Union's Horizon 2020 research and innovation programme under grant agreement No 862253.

Document history

Version Number	Date of issue	Author(s)	Brief description of changes
V 1	11/09/2020	Sambal S Ambu (CENmat) Miriam Goll (CENmat)	Creation of 1st version
V 2	25/09/2020	Stefania Siracusano (CNR-ITAE) Maria Retuerto (CSIC) Sambal Ambu (CENmat) Seyed S Hosseiny (CENmat)	Review and Redaction of 2st version
V 3	28/09/20	Antonino Arico (CNR-ITAE) Maria Retuerto (CSIC) Anastasia Moschovi (Monolithos) Sambal Ambu (CENmat) Seyed S Hosseiny (CENmat)	Review and Redaction of 3rd version

Table of Content

List of Figures

List of Tables

Acronyms

BET - Brunauer Emmett-Teller
BoT – Beginning of Test
CNT – Carbon nano tube
MWCNT – Multiwalled Carbon nanotube
SWCNT – Singlewalled Carbon nanotube
CE - Counter Electrode
CRM- Critical raw material
CV - Cyclic Voltammetry
DHE- Direct hydrogen Electrode
DMF- Dimethylformamide
ECSA- Electro chemical surface area
EDX- Energy-dispersive X-ray
EIS- Electrochemical Impedance Spectroscopy
GCE- Glassy Carbon Electrode
HER- Hydrogen Evolution Reaction
ICP- Inductively Coupled Plasma
OER- Oxygen Evolution Reaction
OCP- Open circuit potential
MMO- Metal/metal oxide
MEA- Membrane electrode assembly
NSTF-Nanostructured thin films
NMP- N-Methyl-2-pyrrolidone
PEM- Proton Exchange Membrane
PEMWE- Proton exchange membrane water electrolysis
PGM- Platinum group materials
PND- Powder neutron diffraction
RDE -Rotating Disk Electrode
RHE- Reversible Hydrogen Electrode
SEM- Scanning Electron Microscopy
SS- Stainless Steel
TEM -Transition Electron Microscopy
TOF- Turn over frequency
XAS- X-ray absorption spectroscopy
XPS- X-ray Photoelectron Spectroscopy
XRD- X-ray Diffraction
XRF – X-Ray fluorescence spectroscopy
WE - Working Electrode

Executive Summary

Among the marketable electrolysis technologies available, proton exchange membrane water electrolysis (PEMWE) technology is the most promising one due its low footprint, compactness, simplicity, wide range of operation, fast dynamics, safety, high hydrogen purity and the possibility of reaching high differential pressures. However, the main drawback of PEMWE technology is the high cost of the materials and components used in the stack. Currently, only a few materials can be used for the operation in the harsh acidic environment of PEMWE. These include critical raw materials (CRM), such as iridium and platinum. WP1 has as overall goal the development and production of advanced catalysts based on ultra-low loading CRM and non-CRM for anodes and cathodes to replace or drastically reduce the CRM content of anode and cathode catalyst layers in PEMWE while maintaining SoA performances and durability.

In scope of this deliverable electrochemical protocols have been defined for setting reference baseline and as a screening method for material. To produce advanced catalysts, existing synthesis routes have been investigated or new synthesis routes have been developed. Initial physiochemical and electrochemical characterization and evaluation has been done for the down selection of materials at lab scale.

1 Introduction

The Deliverable 1.1 report consists of a thorough literature research and down selection of promising materials as electrocatalysts for water electrolysers as well as a harmonized characterization protocol of catalyst testing that will ensure a proper and goal-oriented selection of catalysts and its development. The risks associated with the development of the catalyst are also a part of this report.

The literature research section of the deliverable leads to a broad overview and deep insight of promising materials for reduced CRM and CRM free catalyst for OER and HER. Following this a down selection of potential materials is performed. Broader and deeper survey of materials from an enormous material pool ensures that the material selections are in alignment with the general project objectives. This document also consists of indicative routes of synthesis of the down selected materials. A great attention has been parted specifically towards assessment of the risks related to the development of reduced and free CRM catalysts and their mitigation strategies through backup catalysts development. This also grantees the compliance with the EU's regulations and classifications on critical raw materials.

To allow a harmonized characterization of materials that will ensure a proper and goal-oriented selection of catalysts, characterization protocols are developed. For this, several testing methods are envisioned at lab level to characterise and evaluate the materials. General aspects on procedures and key performance indicators to ensure that the results are comparable and suitable for the down-selection of materials. To compare the catalytic activity between different catalysts electrochemical techniques such as cyclic voltammetry, EIS, rotating disc electrode measurements, etc. and their boundary conditions (catalyst loading, potential range, rotating speed, temperature, electrolyte composition, pre-conditionings…) are defined as part of the harmonised characterisation protocol. In addition, accelerated stress test protocols such as potential cycling, prolonged operation at high potentials to evaluate the degradation of both catalyst active phase and support also have been envisaged in the document.

Additionally, ante and post-mortem physio-chemical characterization test is defined to further shed light on the stability of the materials.

All these procedures should be used as means of verification to assess the achievement of project objectives and milestones.

2 Literature Review

Critical raw materials (CRM) such as Pt, Ir and Ru are currently used as catalyst for the hydrogen and oxygen evolution reaction (HER and OER) due to the harsh environment of PEMWEs. The high costs, the supply risks due to the scarcity and the environmental issues represent drawbacks to overcome in order to reduce costs and environmental impacts and to promote PEMWE technology. The task 1.1 has been started with a thorough literature research leading to a broad overview and deep insight of promising materials for reduced CRM and CRM free catalyst for HER and OER in acidic environment. Following this a screening of the potential materials is performed.

2.1 CRM *reduced* Catalysts

2.1.1 Oxygen Evolution Reaction (OER)

The state-of-the art OER catalysts for water splitting are all based on iridium, which comes at a huge cost of just under 50 k€/kg. In addition to the cost, Iridium is also one of the scarcely available metals in the nature which is a significant roadblock for the sustainability of this technology. CRM loading in PEMWE is with approximately 2-3 mg cm^{-2} too high to meet the long-term cost targets for energy markets. In one hand, reduction of precious metal/CRM loading is significant and in the other hand enhancement of catalytic stability is of equal importance to make the technology economically viable. Long-term operation at high current density up to thousands of hours is particularly challenging with an Ir loading less than 1 mg cm^{-2}. The balance between activity and stability for Ir-based OER catalysts is relevant and it strongly depends on the chemical nature of the oxide and its surface properties.

One strategy to reduce the amount of CRMs includes minimisation of the precious metal catalysts to a level comparable to that of the automotive fuel cells (< 0.2 mg cm^{-2}; <50 €/kW) that have already reached the phase of commercialisation. Nano-structured thin film (NSTF) catalyst-based electrolysis cell have been demonstrated for 5000 h with a constant current load of 2 A cm^{-2} and 0.25 mg/cm^2 Ir loading.[1] IrOx catalyst, prepared by flame-based reactive spray deposition, has also achieved ~4500 h operation in single cell electrolyser at 1.8 A/cm^2 and 80 °C with ultra-low iridium loading of 0.08 mg/cm^2. However, the degradation rate appears still significantly higher than the industry standard of less than 5 µV/h.[2] The degradation rate increases proportionally with the operating turn-over frequency (TOF) or the site time yield (number of evolved oxygen molecules per second on a single catalytic site) of the anode catalyst in a PEM electrolysis cell. Catalyst operation at high turnover frequency was observed to cause a progressive change of Lewis acidity characteristics with time for both Ir and Ru cations thus influencing their ability to promote water oxidation. This evidence clearly indicates the impossibility to achieve stable operation with low catalyst loadings for the present unsupported Ir-based catalytic systems.[3]A change in strategy is required by involving supported catalytic systems and stabilisation strategies in order to significantly increase OER activity and stability of the Ir-based catalysts.

In recent years, DLR has addressed the catalyst problem in PEMWE by developing cost-effective materials with high activity-iridium mass ratio. Amorphous IrOx nanoparticles were synthetized, displaying a 10-fold higher oxygen evolution activity than commercial Ir-black.[4] Further activity increase was

demonstrated for Ir electrocatalyst derived from an amorphous IrRuOx via an electrochemical route, exhibiting 13 times higher OER activity compared to the rutile phase of $Ir_{1-x}Ru_xO_2$.[5]
Enhanced OER activity of vertical aligned IrOx nanoarrays was correlated to the surface area of exposed nanoparticles and to the improved ion transport, performing almost the same current density of commercial IrO_2 NPs with only 1/20 Ir loading amount.[6] In separate instance Rozain and Pham et al.[7] used micro-sized titanium particles as support for IrO_2 nanoparticles in PEMWE achieving 1.73 V at 1 A cm^{-2} and 80 °C. Metal loading of 0.1 mg cm^{-2} of IrO_2 as anode catalyst along with 50 wt.% of metallic Ti has allowed to obtain similar performance with respect to the conventional loadings of several mg cm^{-2} of IrO_2 at the anode side. [8] Notably superior performance was demonstrated by core-shell IrO_2@TiO_2 catalyst compared to commercial benchmark IrO_2 and IrO_2/TiO_2 catalysts with 3-fold higher loadings.[7] It also has been shown that application of advanced electro-ceramic supports such as Ti_4O_7 [9]and SnO_2:Sb-aerogel[10], Sb-doped SnO_2 microparticles[11], has enables the usage of Ir to be decreased by more than 70%, while keeping the same activity and significantly enhancing the stability compared to its unsupported counterpart.

2.1.2 Hydrogen Evolution Reaction (HER)

Pt is the benchmark material used as cathode catalyst in PEM electrolysers (for instance, Pt black and other Pt alloys registered by Tanaka Corp., Johnson & Matthey, and BASF). The HER reaction in acid media on Pt surface is very fast and consequently low Pt loadings are found in electrolysers [12] however, even in low amounts, Pt is still expensive and scarce for large-scale commercialization, so several strategies are being followed to increase the Pt efficiency or finding substitutes without precious metals.
The most common strategy is to reducing Pt particle size, that is to say by increasing Pt dispersion and thus increasing the number of Pt accessible active sites.[13] Usually this strategy is performed by using (high area) carbon supports. Carbon materials suit as catalyst support owing to properties for instance stability in both acidic and basic electrolyte, good conductivity, and high surface area for dispersion of metal catalyst. Various types of carbon black supports are available commercially. Recently carbon nanotubes have gathered much attention as support material for noble metal catalysts because they usually possess superior electron conductivity and corrosion resistance compared to carbon blacks. CNT properties can also be customized for enhanced electrocatalytic activity, electrical conductivity and stability with N, P, S and B doping.[14] Graphene also have attracted traction in recent research due to its high surface area for better catalyst/metal dispersion, high electrical conductivity, and good thermal properties.[15] Another strategy is to tailor Pt electronic properties to enhance its intrinsic activity by, for instance, synthesizing bimetallic solid solutions with Re, Co, Ru, Fe, Ni etc.[16] Replacing Pt with other noble metals with tailored morphologies can allow for a more efficient use of active sites. For instance, Pd can be easily modified to grow as nanoparticles or nanosheets with high specific surface area. In this modified structures it is expected that the strength of the Pd–H bonding, that makes H desorption the rate-limiting step in the HER process, is reduced.[17,18]

2.2 CRM free Catalysts

2.2.1 Oxygen Evolution Reaction (OER)

A long-term approach would consist in replacing platinum group metals (PGMs) with stable and active non-CRM materials. The investigation, identification and development of an active and stable CRM-free OER catalysts (based on e.g. nickel, iron or manganese materials with a cost of about 1-2 €/kg) are required to make non-PGM systems stable and active for OER in the presence of protonic electrolyte membranes.

For the anode (OER), a ground-breaking approach consists in the total replacement of CRM by Ti-based catalysts, e.g., $MnTi_2O_4$, doped with silver (non-CRMs). In addition, a moderate risk approach consisting in the severe decreasing of CRM (<0.2 mg cm^{-2}) by designing advanced Ir mixed oxides and Ir oxide/hydroxide may be also considered as backup solution. These formulations aim at providing a cost-effective solution where the active phase is stabilised by forming a solid solution with stable oxide systems. Ag, Mn and Ti are not included in 2017 EU CRM List[19] and have significantly lower cost than Platinum Group metals (PGMs).[1]

As previously reported in literature, Ag doped Co_3O_4 has showed high electrocatalytic performance for oxygen evolution reaction in acidic environment (0.5 M H_2SO_4) exhibiting higher activity and better durability[20]. Ag-doping greatly enhances not only the conductivity but also the stability of electrocatalyst in acidic media. Ti-based spinels can be investigated as catalyst supports for oxygen evolution reaction catalysts in PEM electrolysers since they may show very high conductivities at room temperature (~10-100 S cm^{-1}) although their stability need to be assessed. [21]

Non-PGM catalysts based on Co spinels have been explored for operation in a proton exchange membrane electrolysis environment. The efforts should however be addressed in this project to replace Co (a critical raw element) with Mn and Ti in the spinel structure.

As also evidenced in the literature, the proposed solution to replace CRMs and to enhance stability and activity of non-CRM materials is to combine spinel systems, which are stable in the acidic environment such as $MnTi_2O_4$ with a tailored Ag insertion. With respect to literature results, the approach used in the present project goes beyond by avoiding CRM materials, such as cobalt, while providing a better stabilization for the spinel oxide. This is achieved using a Ti-Mn based spinel where the inserted Ag acts as both dopant and surface promoter, since Ag-doped transition metal oxides seem to be promising alternative mesoporous nanostructures for efficient OER in acid.

---

[1] The latest published (3rd Sep'20) 2020 EU CRM list[71] identifies Ti as a critical raw material.
However at the time, proposal for this project was written and approved in late 2019/early 2020, 2017 EU CRM list[19] was considered in which Ti was not included. Therefore, in this document, Ti containing catalysts or supports will be considered as non-CRM bases catalysts.
Nonetheless consortium is fully aware of the new available 2020 EU CRM list[71] and efforts will be made to try and adhere to the new CRM list.

2.2.2 Hydrogen Evolution Reaction (HER)

A much more aggressive yet risky strategy is to replace CRM (including Pt) altogether from the cathode side. In 2005 Hinnemann et al. [22] reported that the (101) Mo-edge structure in MoS_2 has high HER activity. In 2007, Jaramillo et al.[23] prepared different MoS_2 nanoparticles of different sizes of with the predominance of the sulphide Mo-edges. They reported that the catalytic performance of MoS_2 nanoparticles is related to the edge state length, rather than the area coverage, directly establishing the relationship between MoS_2's edges and the catalytic active sites. After those findings, many works have been reported confirming the high catalytic performance MoS_2 for the HER.[24,25] Also, several approaches have been undertaken to improve its activity;
(i) Increasing the number of exposed active sites,
(ii) Enhancing the reactivity of active sites, or
(iii) Improving the electrical contact to active sites.
The electronic conductivity engineering can be achieved by two ways:
(i) Doping suitable heteroatoms into the lattice of MoS_2 and
(ii) Coupling MoS_2 with conductive species, such as carbon nanotubes and graphene.[26–28]
It has been reported that doping MoS_2 with Ni, Fe or Co improves its HER performance. In fact, Ni, Co and Fe sulphides present comparable HER performance than MoS_2 by themselves.[29] Therefore, Fe and Ni sulphides are promising catalyst for the HER since they are earth abundant, non-expensive, resistant to sulphide poisoning, and depending on its morphology, present high HER performance. Kong et al.[30] found that both FeS_2 and NiS_2 (pyrite) were active non-precious HER catalysts in acidic electrolyte. FeS_2 and NiS_2 have comparable catalytic activity towards HER, but FeS_2 has higher stability in acidic solution. Moreover, FeS_2 exhibited a higher catalytic activity than the analogous selenides and tellurides. Fe-based sulphide catalysts still have lower catalytic activity than MoS_2, however, in view of their natural abundance; it is significance to search for high performance Fe-based sulphides.[30] Peron et al.[31] carried out a detailed study to compare the performance of FeS_2, Fe_3S_4 and Fe_9S_{10} electrocatalysts for proton exchange membrane (PEM) electrolysers and concluded that FeS_2 is the most active sulphide. The stability of FeS_2 nanoparticles at different pH was reported on [32]. In this work, they found that FeS_2 is reasonably stable in acid media. Several approaches will be followed in this project to improve the HER activity of FeS_2 in acid media such as (a) modify FeS_2 morphology, (b) FeS_2-supported on conductive carbon structures and (c) metal-doped (Co and Ni) FeS_2. There are several previous studies demonstrating the advantages of the approaches:
(a) Tuning FeS_2 morphology.
FeS_2 disks present elevated HER activity in acid media[33]; mesoporous FeS_2 nanoparticles also present promising performance in alkaline media[32] FeS_2 nanoparticles were reported with a Tafel slope of 65 mV/sec, an overpotential of 240 mV at 4 $mAcm^{-2}$ and stable during 1000 HER potential cycles ; and with a Tafel slope 76 mV dec^{-1} in acid media.[33]
(b) FeS_2-supported on conductive carbon structures.
FeS_2/C immobilized on Ni foam has been proved as active bifunctional catalyst for HER/OER. For the HER it was reported an overpotential of 202 mV at 10 $mAcm^{-2}$ being stable during 100 cycles, with an overall water-splitting process of 1.72 V at 10 mA cm^{-2}.[34] FeS_2 nanoparticles embedded in rGO (reduced graphene oxide) display an overpotential of 139 mV at 10 $mAcm^{-2}$, a Tafel slope of 66 mV dec^{-1}, and long-term stability in acidic conditions.[35] Hexagonal FeS_2 nanoclusters embedded in a rGO matrix prepared by hydrothermal synthesis reached a Tafel slope of 61 mV dec^{-1} and stability during 36 h at 200

mV in acid media.[36] The hybrid electrocatalyst FeS_2@MoS_2/rGO exhibits excellent HER activity and outstanding electrochemical durability in acid media, with an overpotential of 123 mV at 10 mA cm^{-2}, a Tafel slope of only 38.4 mV dec^{-1} and excellent stability.[37]

(c) Metal-doped (Co and Ni) iron sulphide materials.

Since Co is a CRM, we will first focus on the doping of Fe sulphides with Ni. Ultrathin nanosheets of NiFeS with abundant pores and vacancies, and therefore increased number of active sites, have reported to have a high HER activity in acid electrolyte, with an overpotential of 81 mV at 10 mA cm^{-2}.[38] Its stability has been studied in alkaline media, being stable during 2000 cycles. In this medium, it records 208 mV at 10 mAcm^{-2} and a Tafel slope of 109 mV dec^{-1}.[39] $Fe_3Ni_6S_8$/NC reaches 196 mV at 10 mA cm^{-2} and a Tafel slope of 55 mV dec^{-1}. [40] NiFeMoS records 210 mV at 10 mAcm^{-2} and a Tafel slope of 88 mV dec^{-1} in alkaline media.[41] Finally, $FeNi_xS_2$-rGO (x = 0.05–0.3) yields lower Tafel slope, smaller electrochemical impedance and reduced overpotential than FeS_2/rGO with an overpotential of only 42 mV at 10 mA cm^{-2} and a tafel of 72 mV dec^{-1} in 0.5 M H_2SO_4.[42]

Electrocatalysts as $FeNi_xS_2$-rGO in which very low overpotentials have been found in acid media makes it worth to try Ni doping on FeS_2. However, most of the studies with Ni have been performed in alkaline media, since Ni is not very stable in acid media. Therefore, although Co is a critical raw material, the activity of FeS_2 clearly increases with Co doping and its stability is, at least, maintained. For instance, in [35] the authors presented a comparison of different Fe-Co doping sulphides, finding that the HER activity in 0.5 M H_2SO_4 goes from an overpotential of 139 mV for FeS_2 or 140 mV for CoS_2, to 120 mV for $Fe_{0.9}Co_{0.1}S_2$ and 69 mV for Co:FeS_2:CoS_2, at 10 mA cm^{-2}. This last catalyst is ultrafine Co: FeS_2/CoS_2 heterostructured nanowires (NWs) formed on carbon fiber paper, which were prepared by a facile hydrothermal route. The HER in acid electrolyte was 69 mV at 10 mAcm^{-2}, Tafel slope of 46 mV dec^{-1} and a shift of only ~ 3 mV over 1000 cycles.[43] In[44] the authors proved the enhancement in HER activity of the Co-doped FeS_2 structures in comparison to undoped FeS_2 with $Fe_{0.5}Co_{0.5}S_2$ supported on oxidized Ketjenblack, that presents an overpotential of 150 mV at 10 mA cm^{-2} and only decreased by 1 mV after 500 catalytic cycles. Also Co doping in highly dispersed FeS_2 (ca. 5 nm size) on ordered mesoporous carbon enhanced the HER to 92 mV at 10 mA cm^{-2} and Tafel slope of 59 mV dec^{-1}.[45]

3 Material Synthesis Strategy

3.1 CRM *reduced* Anode Catalysts:

Pursuing the strategy of using a support material to improve the catalytic activity and stability of the catalysts for the OER will allow a significant reduction of the CRM by depositing the catalyst of top of support materials thus increasing the surface area. These support materials can be effective via two different mechanisms which are *redox couple mediated OER* and *water dissociation reaction*.

For the first mechanism for redox couple mediated OER based on the support materials, the approach combines both chemical and electrochemical reactions. In case of water electrolysis such as constellation should possess however, the redox potential of the redox couple below the electrochemical water splitting potential of the catalyst to act as a mediator. Amstutz et al.[46] & Mills et al.[47] described the OER to be managed via a mediator being a soluble redox couple of CeO_2 (e.g. Ce^{3+} / Ce^{4+} Ions). Such a mediator has the benefit that the OER will proceed significantly faster compared to typical electrochemical route. The choice of a starting support material will be cerium oxide[48,49] due to its redox potential as mentioned earlier which need to be below the redox potential of the actual electrochemical potential of the catalyst for the OER. The systems described in the above cited works contain soluble redox couples, which is not directly applicable for a real PEM electrolysis application due to potential crossover issues of the redox couples through the membrane. Therefore, it is envisaged to apply this methodology to

a) solid and non-soluble redox couples and

b) if possible, to different non-CRMs to achieve the lowest use of CRM, especially PGMs.

Mills et al. shows the relief from the anodic oxidative stress on the ruthenium with cerium mediated OER, which leads in system without mediator to the ruthenium's dissolution and make this material less useful. However the redox potential of Ce^{3+} / Ce^{4+} is quite strongly modulated by the attendant solvent phase as reported by Reed et al[48], it ranges between 1.28-1.74V (vs RHE) in different acidic electrolytes. However, since Reed[48] and Walsh[49] are only referring to soluble cerium ions the redox potential of the Ce^{3+}/Ce^{4+} will be only dependant on the surface concentration of Ce^{3+}. At the bulk scale, cerium oxide can exist as pure CeO_2 (Ce^{4+}) or Ce_2O_3 (Ce^{3+}). Yet, at the nanoscale, cerium oxide contains a mixture of Ce^{4+} and Ce^{3+} at the surface. As the diameters decreases from 20 nm to 2 nm, there is a measurable loss of oxygen atoms and an increase in the number of Ce^{3+} sites on the NP surface.[48] Therefore, it is aimed to synthetize cerium oxide nanoparticles with a size below 5 nm in order to allow high Ce^{3+} coverage thus the redox reaction will be more sustainable and not hindered through the particle size. This is therefore in agreement with our foreseen task to synthetize rather small nanoparticles to increase the surface Ce^{3+} concentration.

To prove this strategy of solid redox couple cerium oxide can be used for the OER as a starting support material with a ruthenium oxide catalyst, which can be deposited onto of it. Cerium oxide, especially CeO_2 will be synthetized by wet chemical synthesis route. For the next stage, a metal salt (Ir/Ru) will be introduced and deposited on the cerium oxide. This will in turn provide the catalyst in which the Ru/IrO_x is supported by CeO_2.

The second mechanism is based on support materials for water dissociation. As a starting support material, TiO_2 will be evaluated first, as it has been proposed to be highly effective for this type of reaction in its anatase phase.[50] It is reported that Ti4c-O2c pairs with a different orientation located at the ridges delimited anatase TiO_2 (101) surfaces show a significant increased hydroxyl formation. This is due to their high acidity/basicity combination and a stabilization effect associated to the chemical bonds of the hydrogen atoms. However, in order to make use of this property without any issues of stability the nanoparticles of the anatase phase need to be around 14 nm as reported by Zhang et al.[51]As OER catalyst, CENmat's iridium nano would be employed in this approach and deposited on the TiO_2. In case the ohmic resistance of the catalyst layers is still too high, then the TiO_2 may be chemically doped with W, $Ti_{1-x}W_xO_2$[52], to reduce the bandgap of TiO_2, and have the right balance between the creation of the hydronium and hydroxyl ions and electronic conductivity. TiO_2 may be synthesized via a hydrothermal synthesis route where a solution of Titanium isopropoxide with ethanol and water will be prepared through hydrothermal reaction.[53] In the next step as desired Ir/Ru salt solution will be deposited on the TiO_2 to provide supported catalyst.

Another concept of using mixed oxides, with reduced Ir content is also looking promising. For instance, perovskites with one B site occupied by Ir and the other by a non-CRM transition metal [M], i.e., A_2MIrO_6. CSIC partner has already prepared and tested this type of double perovskites, in particular Sr_2MIrO_6 (M= Ca, Mg, Ni, Zn…) with high catalytic performance to the OER in acid media. Depending on the pure iridium-based reference materials Sr_2MIrO_6 can outperform the OER activities by far with noticeably lower Ir content. For instance, similar OER performance is achieved by Sr_2CaIrO_6 (ca. 4 µg Ir cm^{-2}) than by IrOx-Ir, currently one of the best OER catalyst reported (10.2 µgIrcm^{-2}). [54] The current density and mass activity of M= Ca and Mg (97 and 31 Ag^{-1} @ 1.48 V) are higher than that of benchmark Ir phases. In order to improve stability, PROMET-H2 aims to prepare catalyst with La in the A position, which is known to be less prone to dissolution than alkaline metals.

In another approach, Ru oxides will be investigated, as they present the lowest overpotentials among OER catalysts; however, they are very unstable since Ru^{4+} oxidizes with the potential to soluble $Ru^{>4+}$ phases. [55] Preliminary results from CSIC partner show an improvement on $SrRuO_3$ activity and stability by Na doping, due to the generation of stable $Ru^{4+}/^{5+}$ mixed valences in the perovskite.[56] Phases with very low Ru content and enhanced durability will be studied by controlling Ru oxidation state and environment.

3.2 CRM *reduced* Cathode Catalysts:

In sync of the previously described section of redox mediated support of OER catalysts, V(II)O can be used as cathode redox mediator support. Amstutz[46] uses the V^{2+} / V^{3+} couple as interacting protagonists with the cathode. The actual HER however happens when the V^{2+} interacts with a non-noble metal catalyst (Mo_2C) and the H^+ to form H_2. This allows using reduced CRM free catalyst for the HER. For the HER the starting support material will be made from vanadium-based materials like the highly conductive vanadium (II) oxide (VO) nanomaterials. As catalyst for the HER, it is envisaged to make use of Pt.

This combination as in the OER case will be serving to validate the effectiveness of the strategy of the solid redox couple support materials. For the synthesis of V(II)O, first V_2O_3 powders will be prepared by prepared by a facile one-step hydrothermal method using a vanadium source.[57] In the next step as synthesized V_2O_3 will thermally evaporated to in a tube furnace to give V(II)O. [58]

Water splitting support materials will also be used for reducing the Pt loading of the material. As already described in the Reduced CRM anode material section TiO_2 splits the water thus increasing the ionic concentrations. For the HER catalyst it is envisaged to start with platinum deposited on top of the TiO_2. The platinum will be deposited on the TiO_2 via a CENmat developed route, ensuring a homogeneous distribution of the platinum on the TiO_2 to allow full utilization of thee platinum and the TiO_2 surface.

In a later stage Mo_2C will be a candidate, among many other possible candidates, as catalyst replacing the Pt. The nano porous molybdenum carbide nanowires will be prepared through precipitation. The product will be filtered, dried subsequently calcined in an argon flow and finally, stored in a vacuum desiccator.[59,60]

A less risky strategy is to eliminate Pt and any other PGM elements from the cathode but keeping the presence of other very active CRM elements (for instance Co or P). The most active non-PGM catalyst reported to date is Ni_5P_4 with η= -0.023 V @ 10 mA cm^{-2}.[61] In general, phosphides present very high HER activities in acid media. Ni_2P was found to deliver an excellent HER activity, with low onset potential, low Tafel slope, and high exchange current density, reaching 100 mA cm^{-2} with an overpotential of 180 mV.[62] Other earth-abundant metal phosphides are also highly active to the HER; for instance, CoP, MoP, WP and FeP nanoparticles, with Tafel slopes between 46 and 50 mV dec^{-1}.[63–66] It has been also demonstrated that the phosphorous and metal content are relevant for the HER. For instance, [67] suggests that phosphide with higher P content exhibits higher performance, following the trend $Ni_{12}P_5 < Ni_2P < Ni_5P_4$. In this sense, we are also focused on preparing the most promising catalysts for HER without PGM elements such as Ni-P phases (Ni_5P_4 and Ni_2P).[68] We expect to achieve overpotentials of ca. 0.023 and 0.04 V vs. RHE at 10 $mAcm^{-2}$ in RDE.

In PROMET-H_2 we will explore the most promising strategies for the synthesis of PGM-free HER catalysts. We will synthetize HER catalysts with advanced morphologies, e.g. Pd-nanosheets and aerogels. These phases are reported to display very high specific surface area and a high fraction of (low-coordination) defect sites (kinks, edges) resulting in materials with high intrinsic activity for certain electrocatalytic process.[69] We will also focus on the most promising catalysts for HER without PGM elements such as Ni-P phases (Ni_5P_4 and Ni_2P).[68] We expect to achieve overpotentials of ca. 0.023 and 0.04 V vs. RHE at 10 mAcm-2 in RDE.

3.3 CRM *free* Anode Catalysts

For the oxygen evolution reaction (OER), highly efficient and stable nanostructured transition metal oxides and alloys based on non-CRMs Ag-Ti catalysts with high surface area will be developed. Advanced CRMs formulations include Ag-doped or Ag-substituted Ti-spinel (Ag-$MnTi_2O_4$), Ag doped Ti-suboxides and nanosized Ag-Ti alloys. Improved durability for the active phase consisting of silver (I) oxide in the protonic environment is achieved by developing solid solutions with stable Ti structures, such as spinel and sub-oxides, characterized by proper conductivity. Anode catalysts will be prepared by electrospinning to obtain nanowire mesoporous morphologies, characterised by enhanced electronic conductivity and reduced mass transport, and by wet chemical methods combined to ball milling. The aim is to

achieve nanosized particles and nanowires with a diameter in the range of 20-50 nm and BET surface area > 150 m^2/g. The electronic conductivity of $MnTi_2O_4$ spinel is sufficiently good for this application (>30 S cm^{-1} in a wide temperature range from ambient to 90 °C) but it can be further enhanced by doping the oxide substrate with silver.

For the non-CRM anode catalyst, Ag is used at low contents (10 %) to activate the process of water adsorption at a stable titanate substrate. Formation of O-O bonds is improved through tailoring of the interatomic distances (insertion of Ag into the $MnTi_2O_4$ spinel causes an increase of the crystallographic unit cell size resulting into larger lattice parameter), while affecting the surface energy and introducing electronic levels into the bandgap of the spinel oxide. This greatly enhances the electronic conductivity. Formation of mesoporous nanowires arrays using an electrospinning preparation procedure further improves the electronic percolation through the catalytic layer. A similar approach has been very recently reported in the literature showing both good performance and conductivity for an Ag/Co_3O_4 electrocatalytic system for oxygen evolution in acidic (0.5 M H_2SO_4) environment[20]. However, the approach used in the present project goes beyond by avoiding CRM materials, such as cobalt, while providing a better stabilization for the spinel oxide. This is achieved using a Ti-Mn based spinel where the inserted Ag acts as both dopant and surface promoter. As also evidenced in the literature, it appears that Ag-doping greatly enhances not only the conductivity but also the stability of electrocatalyst in acidic media[7]. The activity of this specific route is thus addressing a complete replacement of critical raw materials (CRMs) in PEM electrolysers with highly efficient and stable nanostructured high surface area transition metal oxides and alloys based on CRM-free Ag-Ti catalysts. The goal is to achieve an activity > 0.6-1 A cm^{-2} at 1.8 V RHE (IR-free) and a mass activity of 100 Ag^{-1} at the same voltage efficiency, which is significantly higher than the current industrial benchmark for non-noble OER electrocatalysts, whilst avoiding the use of CRM materials such as iridium and ruthenium. The aim is also to limit the CRM-free catalyst loading to less than 5 mg cm^{-2}.

3.4 CRM *free* Cathode Catalysts

The cathode catalysts will be based on Fe and Mo sulphides and nitrides. Through optimizing the morphology and composition, the catalytic performance and stability towards the HER are foreseen to be enhanced. In a first approach, the fraction of edge sites will be increased through the control of the particle size. This strategy has been proved successful to enhance HER performance of MoS_2. Also, coordination number (CN) of the active metal has been reported to govern the HER. Thus, surface (100) planes in FeS_2 exhibit square-planar co-ordinations (CN=4) with S-Fe-S terminations are more active to the HER than FeS_6 octahedra (CN=6). FeS_2 with different morphologies will be synthetized to favour the formation of these active surfaces, for instance, by growing nanoparticles, nanowires or nanosheets. Mesoporous FeS_2 with an overpotential of ca. 0.1 V (vs RHE) at 10mAcm^{-2} has been reported. The synthesis of these MoS_2 and FeS_2 materials with enhanced HER activity and durability will be realized through techniques such as microemulsion or colloidal techniques. It has been reported that Co and Ni doping can enhance the HER catalytic activity of iron sulphides. In a second approach we will deposit the active transition metals on different supports, for instance heteropoly acid structures.

4 First Developments

4.1 CRM *reduced* Anode Catalysts

As initial anode catalyst with reduced Ir content, *IrRuOx* was synthesized according to the paper[70] by *CENmat*. The herein presented catalysts are synthesized via direct co reduction of Ir and Ru salts protected via a capping agent via a wet-chemical method. A brief synthesis route is as follows. A known amount of anhydrous $IrCl_3$ and $RuCl_3$ salts are dissolved in absolute ethanol to make a homogeneous solution through ultrasonication for 10 min. Amount of salts are adjusted such that the final product will have wt.% ratio of Ir:Ru as 7:3. A second solution of CTAB and absolute ethanol was prepared which was then introduced in the metal salt solution and ultrasonicated for 10 min. After that, the as prepared solution is mixed using a magnetic stirrer. Meanwhile another solution of sodium borohydride ($NaBH_4$) as the reducing agent and ethanol is prepared with the assistance of an ultrasonication bath for 10 min. The reducing agent solution is added at 2–3mlmin^{-1} to the metal salt-surfactant solution which is additionally purged with argon and now mixed at 600 rpm. This co-reduction of metal salts takes place within an hour colouring the solution from greenish to blackish. Solution was stirred for 12 more hours to ensure an entire reduction. Afterwards, the as-synthesized nanoparticles are separated from the liquid phase by a centrifuge. For removing contaminations, the powder is washed four times with ethanol and four times with deionized water as well. Finally, the wet powder is dried in a furnace at 40°C under an air atmosphere.
RDE characterization was chosen as technique to quickly screen the catalytic activity of as synthesized $IrRuO_x$ and to draw an activity comparison to the benchmarking catalyst Iridium black.[2]

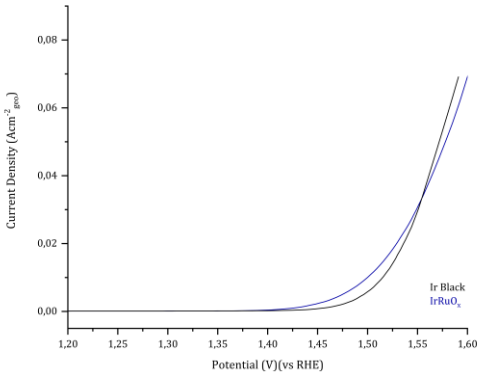

Figure 1 OER activity comparison between Ir black and $IrRuO_x$ catalysts

For quick screening, the important parameter of overpotential at 10 mAcm^{-2} of the catalysts are compared which was found to be 270 mV and 300 mV (vs RHE) for $IrRuO_x$ and Ir black, respectively. As a first glance it can be realised that inclusion of ruthenium into iridium increases the potency towards

[2] RDE was performed at room temperature with 1600 rpm and a catalyst loading of 200 µgcm^{-2} keeping ionomer to catalyst ratio 0.2 in 0.5M H_2SO_4.

OER, on the other hand it also opens the door of making CRM catalysts relatively inexpensive as ruthenium is cheaper than iridium. However, it is a topic of discussion that why inclusion of ruthenium increases the catalytic activity of Iridium. It is also not advisable to reach any conclusion in absence of more rigorous electrochemical and physiochemical characterization. In the next stages as-synthesized catalyst will be deposited on redox mediator and water splitting support to reduce the loading of CRM materials in anode catalysts.

CSIC have explored the strategy of CRM reduction via synthesizing iridium double perovskites. The synthesis approach to prepare Ir perovskites is using the citrate method followed by high temperature treatments (between 800-1100 ˚C). In the oxides where Ir is in a high oxidation state inside the structure (e.g. Sr_2CaIrO_6) then high oxygen pressures are required for the synthesis. As first catalyst Sr_2CaIrO_6 is prepared and characterized.

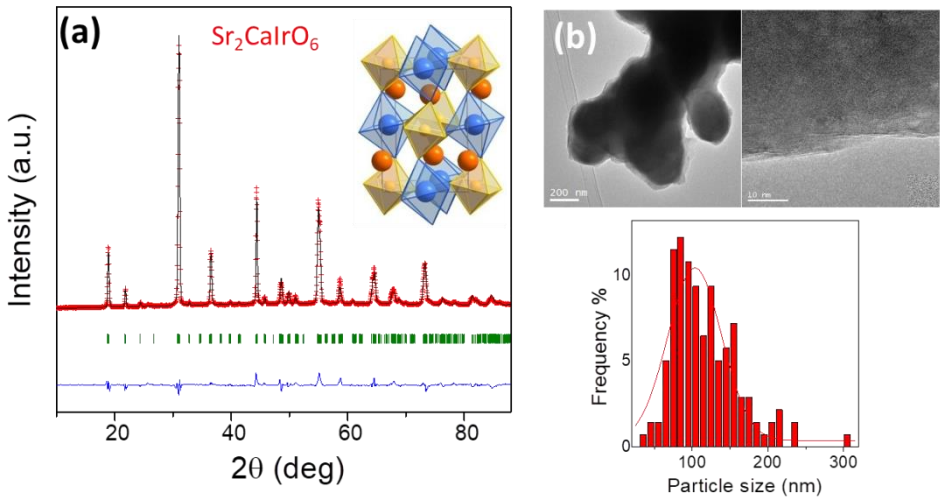

Figure 2 (a) XRD structural refinement of Sr_2CaIrO_6. The inset shows a schematic view of the crystal structure. (b) TEM images of Sr_2CaIrO_6 and particle size distribution.

Figure 2a shows the XRD data of the mixed oxide. The Rietveld refinement of the crystal structure indicates that the mixed oxide is a pure oxide with double perovskite structure and monoclinic space group ($P2_1/n$). Figure 2b shows the TEM and HRTEM images together with a particle size distribution.

In line with the material synthesis strategy ruthenium bases catalysts will also be prepared. The synthesis procedures followed for Ru phases will also be based on *wet chemistry*, trying to lower the final synthesis temperatures and therefore reduce the particle size in order to improve the number of active sites exposed to the reaction.

4.2 CRM *reduced* Cathode Catalysts

CSIC has started working on Ni-P phases and Pd nanosheets/aerogels. Colloidal methods are being used to prepare Ni_5P_4 nanoparticles. In our first trial, Nickel(II) acetylacetonate ($Ni(acac)_2$; Aldrich, 95%) was mixed with trioctylphosphine (TOP, Aldrich, 97%) as a phosphorus source and trioctylphosphine oxide (TOPO; Aldrich, 99%) as a coordinating solvent. The mixture in the flask was heated to 360 °C and refluxed for 1 h in an Ar atmosphere. The resultant particles were isolated by centrifuging the mixture and washed with a mixture of hexane, ethanol and acetic acid (10: 4: 1). On the other hand, also Ni_4P_5

nanoparticles were synthetized using a solid-state procedure. For this route 1.5 mol % stoichiometric excess of P(red) (Alfa - Aesar 99%) and stoichiometric amounts of Ni(s) (Sigma-Aldrich < 150µm) were thoroughly mixed in a mortar. The mixture is introduced into a quartz tube in which is evacuated, sealed under N_2 atmosphere, and heated to 700 °C during 24 h.

Ni_2P nanoparticles have been also reported as good catalyst for HER. Ni_2P will be synthetized by heating nickel (II) acetylacetonate ($Ni(acac)_2$) in 1-octadecene, oleylamine and octylphosphine (TOP) at 320 °C for 2 h. The obtained powder will be washed with ethanol and hexane, and isolated by centrifugation.

In PROMET-H_2 CSIC have also synthetized HER catalysts with advanced morphologies, e.g. Pd-nanosheets and aerogels. These phases are reported to display very high specific surface area and a high fraction of (low-coordination) defect sites (kinks, edges) resulting in materials with high intrinsic activity for certain electrocatalytic process.[69] Pd nanosheets are prepared via reduction methods using CO as reducing agent.

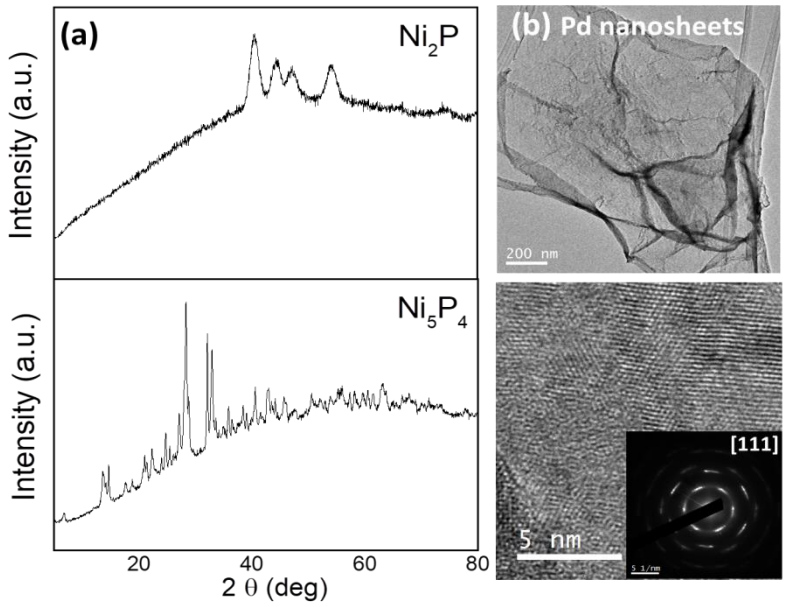

Figure 3 (a) XRD patterns of Ni-P phases. (b) TEM study of Pd nanosheets

Figure 3a shows the XRD patterns of two Ni-P samples. The first one shows Ni_2P structure. The XRD pattern presents very broad reflections indicating the small size of the phosphide particles. On the other hand, Ni5P4 has been also prepared and the XRD pattern is also shown in the figure. The particle size of such phosphide is larger, as it is evidenced by the sharper XRD reflections.

Figure 3b illustrates the TEM study of Pd nanosheets. We are successfully forming very thin 2D nanosheets with the preferential orientation of [111] planes in the surface.

4.3 CRM *free* Anode Catalysts

Synthesis route for *Ag doped* $MnTi_2O_4$ has been established by *CNT-ITAE.* The synthesis route consists of three main steps, namely synthesizing Silver nanoparticles, $MnTi_2O_4$ support and wet impregnation of silver active phase on $MnTi_2O_4$ catalytic support.

Silver nanoparticles were synthesized by reducing $AgNO_3$ (Aldrich, 99.995%) with a weak reducing agent in the presence of ultrasonic waves. 0.1 M silver nitrate solution ($AgNO_3$, Aldrich ACS reagent ≥99.5%) was added to a conical flask in an ultrasonic cleanser (Elmasonic S 100/h ultrasonic device operating at an ultrasonic frequency of 37 kHz and with a power of 550 W). 0.1 M citric acid solution (Aldrich ACS reagent ≥99.5%) was added dropwise to the aqueous solution of $AgNO_3$ in the presence of ultrasonic waves. After the acid addition, the pH has been corrected to ~5.2 and the resulting mixture became dark brown and was further sonicated overnight. The suspension was then filtered, and the precipitate was washed three times with hot ultra-pure water to remove any water-soluble impurities and eventually decompose further citrate-silver complex in the solution. The light grey precipitate was then dried in an oven at 50 °C for 3 h.
$MnTi_2O_4$ was synthesized by solid state procedure starting from analytically pure manganese (II) acetate and titanium oxides (TiO_2 and Ti_2O_3), all the reagents were supplied by Aldrich. The spinel structure was obtained by a two-step process. In a first step, manganese acetate and TiO_2 were mechanically mixed in the molar ratio of 1:1 in a porcelain mortar and were fired together in alumina crucible at 1200°C for 16 hours to obtain $MnTiO_3$. The precursor was then mixed with stoichiometric amounts of Ti_2O_3 and TiO_2. The materials were ball milled in a planetary mill and fired at 860°C for 16 hours to obtain $MnTi_2O_4$.

Ag-doped $MnTi_2O_4$ catalyst was prepared by incipient wetness impregnation method using a 20% wt. % of Silver. Ag nanoparticles were dispersed in water and the Ag-based solution was added to the $MnTi_2O_4$ support. The catalyst was then dried and calcined in oven at 150°C for 1 h to remove the volatile components and to obtain silver oxide nanoparticles on the catalyst surface.
Morphological examination of as prepared Ag-doped $MnTi_2O_4$ catalyst has also been done. High magnification image in the inset shows the homogeneous dispersion of silver oxide nanoparticles on the catalyst surface.

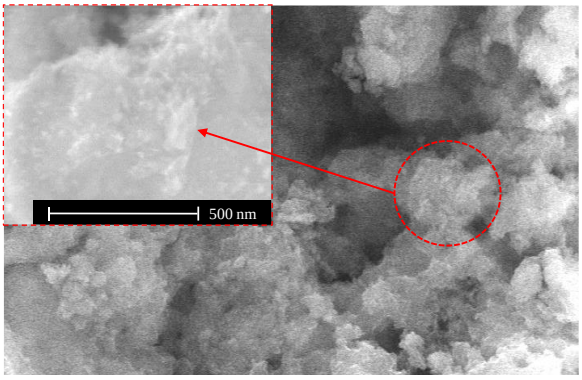

Figure 4 SEM micrographs of Ag-doped MnTi2O4 catalyst at different magnification.

4.4 CRM *free* Cathode Catalysts

The nanoporous molybdenum carbide nanowires (np-Mo_2C NWs) were prepared according to reported method[60] with some modifications by *CENmat*. Typically, ammonium heptamolybdate and aniline were added to distilled water. As the next step aqueous HCl (1 M) was added dropwise to the above solution while stirring the solution magnetically at room temperature until a white precipitate was obtained at pH 4–5. After additionally stirring the solution at 50°C for 6 hours, the product was filtered, washed with ethanol, and dried at 50 °C in an oven for a further 10 hours. After expelling air for 4 hours at room temperature using argon, the products obtained above were calcined at 725 °C for 5 hours in an argon flow in a tube.
Some of the morphological examination of the catalyst are shown in *figure 5 and 6*

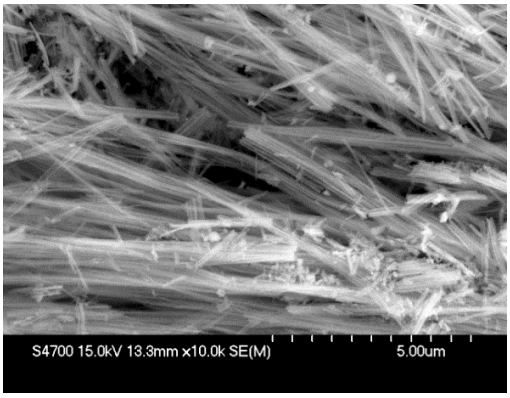

Figure 5 SEM images of Mo_2C catalyst

Figure 5 shows the SEM image of the as synthesised Mo_2C catalyst. Mo_2C catalyst shows needle or wire like shape of the particles with a smooth surface as intended during synthesis.

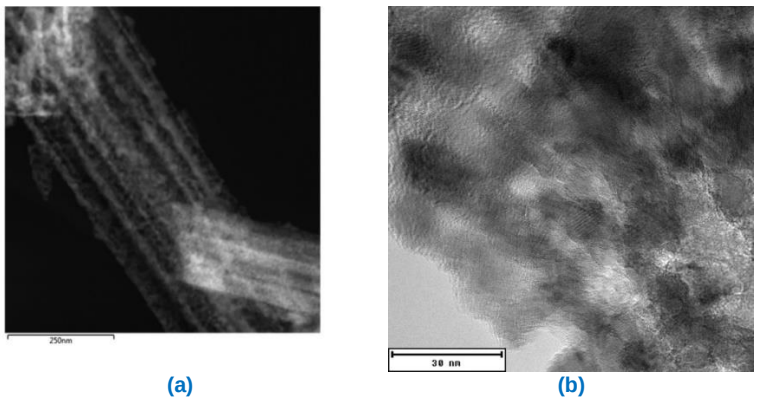

(a) (b)

Figure 6 TEM image of Mo_2C in different magnification

The images shown in *figure 6* are TEM images of Mo_2C in different magnification. In figure 6a the picture on left we can see unilateral alignment of crystallites a typical characteristic of nanowires, while in 6b we can see that the crystallites are small in size (approx. 10 nm).

RDE testing was done to judge HER activity of as synthesized Mo_2C-CENmat and commercially available Mo_2C and comparison was done with @C benchmark catalyst as depicted in *figure 5*. Over potential at 10mAcm^{-2} was found to be 25 mV, 145 mV and 236 mV (vs RHE) for Pt@C, Mo_2C-CENmat and Mo_2C commercial, respectively. As synthesized Mo_2C was found to have impressive catalytic activity for HER when compared to commercially available Mo_2C, but lags in performance to that of Pt.[3]

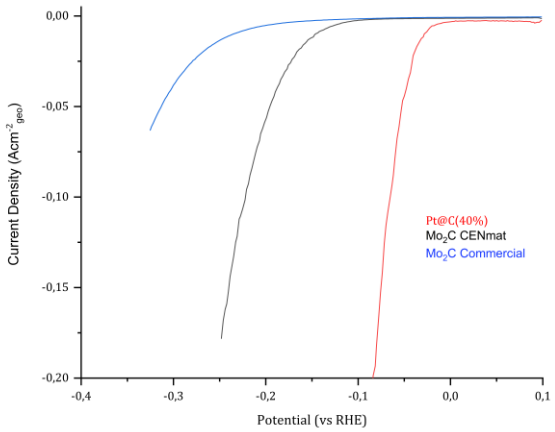

Figure 7 HER activity comparison between Pt@C (40%), Mo_2C CENmat and Mo_2C commercial catalysts

Considering above characterizations, we can safely assume that that uniform one-dimensional morphology, nano crystallite size collectively with large surface area associated with nanowires. All the previously stated features significantly boost the efficiency of the Mo_2C towards HER.[59] In the next stages of the project, Mo_2C-CENmat will characterized deeply and also will be deposited on a redox mediator support namely VO to lower effectively the overpotential..

Parallelly CSIC have started with the synthesis of MoS_2 supported on different carbon structures. A solvothermal synthesis route has been followed for the synthesis of MoS_2 supported on black pearls. As molybdenum precursor, $(NH_4)_2MoS_4$ was mixed with black pearls (2:1) and added to NN-dimethyl. After 10 minutes, hydrazine was added to the solution and the mixture was sonicated for 30 min. In a Teflon container and it was brought to 200 ºC in a furnace for 10 hours. Once it is at room temperature, the solid was recovered by centrifugation, washing three times with MiliQ water and one time with ethanol. CSIC is also exploring various routes for the synthesis of FeS_2 nanoparticles using different salts such as $FeCl_2 \cdot 4H_2O$ (Sigma, ≥99%) or $Fe(NO_3)_3$ (Sigma, ≥99.95%) as iron precursors, and $Na_2S_2O_3 \cdot 5H_2O$ (Sigma, ≥99.5%) and L-cysteine ($HSCH_2CH(NH_2)CO_2H$; (Sigma, 97%) as Sulfur sources. Solvents such as dimethyl sulfoxide (DMSO; Sigma, ≥99.99%) or ethanolamine (ETA; Sigma, analytical reagent, 99%) and thioglycolic acid (TGA; Sigma, ≥99 %) as stabilizers for the formation of nanoparticles are being explored. The synthesis routes are typically being performed between 140°C and 200°C between 12h and 24h under conditions of continuous reflux. The samples formed will be isolated with a centrifuge and several washes were carried out with water and ethanol. Another route that will be followed for the

[3] RDE was performed at room temperature with 1600 rpm at 5 mVs^{-1} sweep rate and catalyst loading of 250 µgcm^{-2} keeping ionomer to catalyst ratio 0.2 in 0.5M H_2SO_4

synthesis of FeS_2 nanoparticles is by Fe_2O_3 sulfurization. Fe_2O_3 will be heated to 150 °C, under H_2S flow and Sulfur powder added as the sulfur sources.

The characterization of MoS_2 and FeS_2 catalysts is currently being developed. However, we have performed the first HER activity measurements for CRM free and reduced cathode catalysts. For the HER studies, a three-electrode cell has been used. As a reference electrode an Ag / AgCl (sat) is used (all potentials are represented *vs.* RHE). A graphite rod is used as a counter electrode and a glassy carbon RDE is used as the working electrode, where the catalyst is deposited as an ink. Catalyst conditioning is performed in Ar-saturated electrolytes by recording 20 cyclic voltammograms at scan rate 50 mVs^{-1} between 0.05 and 1.2 V (vs. RHE) in 0.5M H_2SO_4. For the HER measurements the electrolyte is saturated with H_2 and cyclic voltammograms are recorded at 5 mVs^{-1} and 1600 rpm in a window potential between -0.4 and 0.1 V.

The first HER measurements have been made for MoS_2 and Ni_4P_5 catalysts (*figure 8*). The results show overpotentials of ca. 104 mV and 148 mV vs. RHE at 10 $mAcm^{-2}$ in RDE for MoS_2 and Ni_5P_4 respectively.

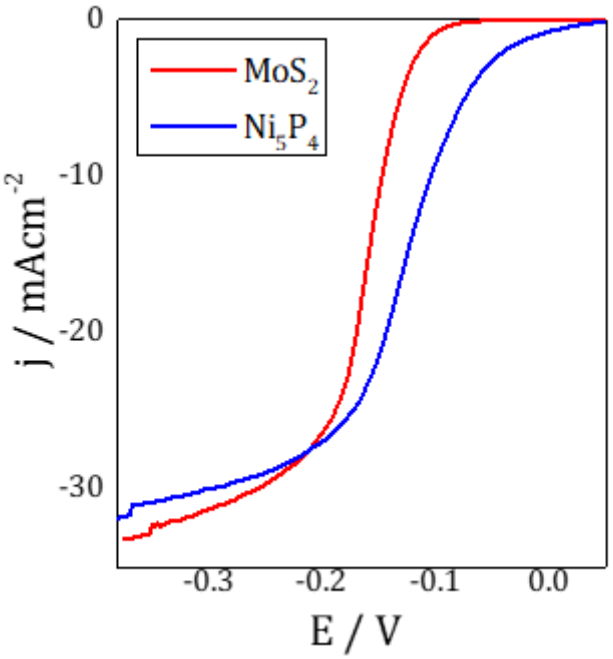

Figure 8 HER activity of MoS_2 and Ni_5P_4 in 0.5 M H_2SO_4 recorded at 5 mVs^{-1} and 1600 rpm

5 Properties of Electrocatalysts

5.1 Physio-chemical Characterization:

The nature of the catalyst including composition, textural properties, phases, surface composition, morphology, number of active sites, active sites environment, oxidation states, defects etc., will be evaluated ante and post-mortem. During the durability experiments, the dissolution of the active phase in the electrolyte will be examined by analysing the composition of the electrolyte by ICP-Plasma.

- Crystal structure information, phase identification, crystalline domain size or unit cell dimensions from Debye-Scherrer equation will be determined through XRD.
- Elemental composition and surface morphology of as prepared catalyst as well as used MEA (without any treatment) for investigating morphological changes, membrane and catalyst layer thinning, particle agglomeration through SEM and EDX.
- Detection of elements at any concentration, detection of possible impurities will be determined through ICP (Inductively Coupled Plasma).
- To determine surface morphology and chemical structure (nature of atoms at surface) before and after use, X-ray photoelectron spectroscopy (XPS) is carried out.
- For surface area measurement and pore size distribution investigation BET (Brunauer Emmett-Teller) measurement will be used.
- TEM (Transition Electron Microscopy) will be carried out to assess the mean particle size, particle size distribution of as prepared and used catalyst also the changes in the parameters will be investigated. Identical Location-TEM may also be used for precise investigation of changes in catalyst post use.
- PND (Powder Neutron Diffraction) technique may be very useful to characterize the crystal structure of CRM-free catalysts elements, being a powerful technique for a detailed characterization of sulphides, oxides, phosphides etc.
- To determine the environment of the atoms in the catalysts (ante and post-mortem) such as coordination number, oxidation states and bond distances. Hard and soft X-rays can be used to study heavy elements and light elements, respectively XAS (X-ray absorption spectroscopy) may be used.
- In addition, XRF (X-ray fluorescence) may also be carried out to determine chemical modifications.

5.2 Electrochemical Characterization

5.2.1 Materials and Methods

Screening of catalysts are carried out through half-cell, RDE and single cell measurements in the presence of standard reference electrolytes and polymer electrolyte membranes developed in the project ***Half-cell investigation*** will be carried out regarding both anodic and cathodic reactions to evaluate individual activation overpotentials, stability in acidic environment and electrocatalytic activity. Below is the measurement condition and available options and values are described:

Table 1 Measurement conditions for Half cell

Parameters	Selected values
Electrolyte Solution	0.5M H2SO4
Temperature of testing	25-80 °C
Bubbling Gas	N_2/Ar
Reference electrode	RHE, MMO, Hg/$HgSO_4$ (all the results will be depicted vs RHE)
Baseline anode	Ti / SS grid with catalytic layer (loading -2-3 mg cm-2 of PGM Ir, Ru, IrOx)
Baseline Cathode	Carbon paper/Carbon cloth (loading -0.5 mg cm-2 of 40% Pt/C,)

At this moment, no base line has been identified for non-critical raw materials since no commercial or standard CRM materials have been identified or are available for the acidic environment. During development of non-CRM catalysts, the appropriate optimum baseline will be selected and used.

RDE is most sought out method to provide a reliable way for screening the performance for HER/OER reactions of novel electrocatalysts. It presents several advantages for instance the amount of catalyst need is small and hold same argument for time for testing the catalyst material, which allows us to test a large amount of catalysts in rapid time.

High purity chemicals (including solvents and gases) should be used. Glassware should be cleaned thoroughly before each experiment. It is recommended to soak cells in concentrated solution of NaOH followed by immersion in piranha solution (98% H_2SO_4 and 30% H_2O_2 in 3:1 v/v) for 24 h followed by rinsing in abundant Millipore water. In all cases, the potential of the electrode should be calibrated before each experiment potentials should be reported vs RHE by considering the offset potential (E_{offset}). E_{offset} is the departure for E= 0.0 V at current = 0 mA), so that E_{RHE}= $E_{measured}$ - E_{offset}.

Table 2 Measurement conditions for RDE

Parameters	Selected values
Electrolyte Solution	0.5M H2SO4
Temperature of testing	25 °C
Bubbling Gas	N_2/Ar

Reference electrode	RHE, MMO, $Hg/HgSO_4$ (all the results will be depicted vs RHE)
Rotation speed	1600 rpm
Counter electrode	Pt wire, Pt foil, graphite bar
Working electrode	GCE

Electrocatalyst testing in single cell will allow carrying experiments in situ and at temperature and pressure conditions which may be not accessible in half-cell. The aim is to assess the catalysts while there are operating inside a MEA Moreover, these experiments will provide information about catalyst/polymer electrolyte interface performance and stability. For diagnostic experiments in single cell dealing with the anode, hydrogen is fed to a Pt/C cathode which acts both as reference and counter electrode. In this specific case, for diagnostic purposes, the Pt loading at the cathode can be significantly large (1 mg cm^{-2}) than the project target to avoid significant polarization of this electrode as required for a reference system. Correction for ohmic drop using ac-impedance, mainly due to the membrane, will allow to determine overpotentials at a specific current. Polarisation curves can be reported as raw curves vs. RHE (or DHE), IR-free curves and Tafel slopes. Overpotentials are determined from IR-free Tafel plots after ohmic resistance correction. This is determined from series resistance in the AC-impedance spectra.

Single cell testing of CRM-free and ultra-low loading CRM cathode catalysts can be carried out using hydrogen pumping cells with the counter/reference electrode fed with hydrogen and containing large Pt loading as reported above to avoid polarization compared to ultra-low loading CRM and non-CRM cathodes.

For a rapid identification of the most promising materials in the pre-screening phase, single cell hardware already available in the partners laboratories e.g. 4 cm^2, 5 cm^2, 8 cm^2 and 25 cm^2, 100 cm^2 may be used. MEAs will be developed by proper methodologies in the Consortium laboratories and discussed with the other partners for cross-comparison. The selected reference membrane is Nafion 117. Alternatively, in some experiments, benchmark Nafion 212 (50 μm) can be used to minimise ohmic losses when this is required.

5.2.2 Catalytic Ink and drying:

Given the diversity of the catalysts that will be prepared and used in scope of this project, the there is no strict guideline for ink and electrode preparation for *half-cell /RDE* measurements. For *half-cell*, the backing layer is cleaned thoroughly with acidic solution and wasted with ultra-pure water. For the preparation of anode as prepared ink in either sprayed, rolled, or spin casted on the backing layer. The electrode is then dried in an oven, heating plate, or leaving in room environment.

For RDE measurements the desired catalyst will be casted on a GCE by means of an ink. The thickness of the catalyst layer should be around 1 μm. The catalyst ink is prepared by dispersing the catalyst in a mixture of solvents.

Some options for preparing the ink are given in the table below.

Table 3 Catalytic ink preparation for Half cell and RDE

Parameters	Selected values
Solvents	Water, IPA, EtOH, DMF, NMP
amount	As required
Ionomer used	Nafion
Ionomer to catalyst ratio (wt.%)	Half-cell-0.25
	RDE-0.2

The composition of the ink cannot be anticipated beforehand since it will depend on the physicochemical properties of the catalyst (surface area, polarity, hydrophobic/hydrophilic balance etc.). Usually, the ink contains solvents such as isopropanol, DMF, ethanol and DI water in different ratios. The addition of Nafion ionomer (e.g. 5 wt. %) is recommended, maintaining an ionomer to catalyst ratio (I/C) around 0.25 for *Half-cell* and 0.2 for *RDE* measurements. A known amount of the catalyst under study is dispersed in the mixture using an ultrasonic bath or probe, during e.g. 20 min. When the catalyst presents low conductivity, (typically oxides or sulphides) it is recommended to add ca. 20 % (weight) of an inert conducting material, typically carbon. Caution should be taken since at high potentials (OER) carbon corrosion can take place.

A known amount of the catalyst ink should be dropped onto the working electrode. For catalysts based on oxides, sulphides, nitrides etc., catalyst loading around 0.28 mg catalyst cm^{-2} disk is known to provide reliable results. To assure and homogeneous deposit of the catalyst on the electrode it is necessary to avoid the preferential evaporation of the solvent at the periphery of the electrode. This can be achieved by the rotational-air dry approach, whereby the catalyst-ink is deposited on an inverted rotator and let dry under rotation.

For inks for single cell test to prepare MEAs depends of the methods to prepare/assimilate the MEAs. Inks will be developed by proper methodologies in the Consortium laboratories and discussed with the other partners for cross-comparison

5.2.3 Protocols for Electrochemical Testing:

5.2.3.1 Electrocatalyst testing in Half cell:

Testing Methods	Description
Polarization Curve	• Change the anodic or cathodic current density in steps as reported in Table 5 (See appendix). • Allow the voltage to stabilise until a steady state conditions are achieved (± 2 mV/min). • If the steady state is not achieved in 2 mins change the step by sampling data and record the corresponding variation. • The cut-off voltage is fixed at 2.0 (vs RHE) for the anode and -0.5 (vs RHE) for the cathode. • At the end of the I-V curve measurements, the current density will be set to zero (OCV).

	• Ohmic resistance is determined from series resistance in the AC-impedance spectra • Polarisation curves are also corrected by the ohmic losses using the series resistance obtained from the ac-impedance tests • E vs Log I to determine Tafel slopes. Overpotentials are determined from IR-free Tafel plots
EIS	• EIS can be carried out in potentostatic or under galvanostatic mode. • In half cell, EIS spectra of the anode can be recorded in potentiostatic mode starting from OCV thereafter at 1.5 V RHE, 1.8 V RHE; under galvanostatic mode at 50 mA cm^{-2} and maximum achieved current. • In the potentiostatic mode, apply a sinusoidal AC perturbation signal with an amplitude (peak-to-peak) of maximum 10 mV and a perturbation frequency in the 1 MHz to 10 mHz range as well as in the reverse order with 10 data points per decade in logarithmic spacing. • In the case of galvanostatic mode, 10% sinusoidal oscillations. The impedance measurements are plotted as Nyquist plots (negative imaginary part vs. real part) and Bode plots (impedance amplitude, real and imaginary part vs. perturbation frequency and/or phase shift). • The cell ohmic resistance is determined from the series resistance i.e. from the high frequency intercept on the real axis. • The polarisation resistance is the difference between the low and the high frequency intercepts on the x-axis of the Nyquist plot.
Cyclic Voltammetry	*CRMs reduced catalysts* • For cathode catalysts cycling in the potential range 0.1 to-1.25 (v RHE) and for the anode catalysts 0.0 to1.8 (vs RHE) with a sweep rate in the range 10-150 mV s^{-1}. • Determination of ECSA for the cathode is made by integration of H adsorption (theoretically 0.210 mC/real cm^2) peaks (0.02-0.4 V RHE) after subtraction of double layer charging at 0.4 (v RHE); whereas for the anode, active area expressed as specific charge q* is obtained from integration in the 0.4-1.4 potential window. *For the CRM-free catalysts* • Similar CV analyses will be carried out after having investigated the stability range of potentials. Some CRM-free catalyst may give raise to faradaic processes in the above reported potential range with irreversible modifications. This should be investigated by CV. Once the stability range is identified, CV are carried out as above

	• Coulombic charges are recorded and used to compare and screen catalyst and interfaces. Coulombic charge q* is obtained from integration in the specific potential window.
Alternatively, the double layer capacitance may be used for non-CRM catalysts. The double layer capacitance is related to the active surface area and is reported as mF cm^{-2} and/or mF mg^{-1}. The capacitance in mC/cm^2 is calculated from AC-impedance, preferably at OCP, and it is divided by the catalyst loading in mg. Deconvolution of the double layer capacitance from the pseudo capacitance can be done using equivalent circuits, this method serves mainly as comparison. The voltametric surface charge is generally considered an indication of the electrochemical active surface area even if a conversion of the charge into surface area is difficult because the nature of the surface reactions is not known precisely.	
Catalyst Degradation	• Accelerated stress tests consisting of potential holding at 2.2 V for 48 h in a three-electrode configuration. Potential holding at -0.5 V vs. RHE for 48 h will be used to test the stability of the cathode in a three-electrode configuration mode. These procedures apply to both reduced CRM (ultra-low loading) and CRM free catalysts. • Dynamic behaviour for catalysts is made by potential cycling. This is carried out preferably in single cell (see below). Eventually, initial tests in half-cell can be carried out by varying the potential between 1 and 1.8 V RHE for the anode and 0 to -0.4 V RHE for the cathode (1 min per step) for 100 – 1000 h. Reference cyclic voltammetry to investigate ECSA loss will be carried out at the beginning and end of the tests (BoT and EoT). This is carried out as reported above for the different catalyst categories.

Reference cyclic voltammetry to investigate ECSA loss will be carried out at the beginning and end of the tests (BoT and EoT). This is carried out as reported above for the different catalyst categories.

5.2.3.2 Electrocatalyst testing in RDE

Testing Methods	Description
Cyclic Voltammetry	*HER Catalysts* • Working electrode cleaning and catalyst condition conditioned in Ar-saturated electrolytes by recording 5-20 cyclic voltammograms at high scan rate (50-200 $mVs^{-1)}$ between 0.05 and 1.2 V (vs. RHE).

	• The electrolyte will be replaced and saturated in H_2 to ensure H_2 saturation so that the potential is not affected by hydrogen evolution. • ECSA may be measure by cycling the catalysts between 0.05-1.2 V (vs RHE) 3 or more times at a scan rate of 20 mVs^{-1}. • A series of cyclic voltammograms will be recorded at 5 mVs^{-1}, 1600 rpm. For the initial catalyst screening, the HER potential window will be selected so that the current density is below 2 mA/cm^2 since higher current densities usually result in the formation of hydrogen bubbles. • The potentials should be corrected by the ohmic resistance • At least, the potential to obtain a current density of 10 mA/cm^2, since this value will be the first benchmarking RDE value to assess the quality of the catalysts. If the catalysts are highly active the potential window can be extended to obtain higher current densities. *OER Catalysts* • Working electrode cleaning and catalyst condition conditioned in Ar-saturated electrolytes by recording 5-20 cyclic voltammograms at high scan rate (50-200 $mVs^{-1)}$ between 1 and 1.7 V vs. RHE). • Electrochemical oxidation and OER activity testing will be done between 0-1.7 V (vs RHE) till the stable CV is obtained. • The potentials will be corrected for ohmic resistance.

However, if at low scan rates the electrochemical signals seem to be noisy and unreliable, the scan rates may be adjusted accordingly.

Key performance indicators (see Table 6 in appendix) will be determined during the testing.

The most accurate way to assess catalytic performances is to determine the intrinsic activity or turn over frequency (TOF), which refers to the number of times the reaction takes place (or number of exchanged electrons) in an active site per time unit. However, the determination of the number of active sites is not straightforward, especially when dealing with non-noble metal-based catalysts. Instead, the metrics usually employed to benchmark catalytic activity are the specific activity (SA) and the mass activity (MA). SA is the activity normalized to the surface area of the catalyst. The surface area of the electrocatalysts is usually referred to as the electrochemical surface area (ECSA) and several methods can be used to determine ECSA of metal catalysts, including H_{upd}, metal UPD and CO_{ad} stripping. However, the determination of ECSA of CRM-free catalysts is challenging.

Methods such as recording adsorption desorption isotherms of gases (typically N_2) usually referred to as BET method allows for obtaining the total specific surface area of the catalysts. Also, catalyst dispersion can be determined from catalyst particle size obtained by TEM assuming spherical particles. Finally, the determination of the area of CRM-free catalysts can be assessed from the double-layer capacitances (C_{dl}) values recorded at different scan rates. According to the equation $i = C_{dl}$. C_{dl} is related to the ECSA via the specific capacitance (in F/cm^2), sadly, specific capacitances are usually unknown.

Catalyst Stability	• Continuous potential sweeps at a scan rate of 50 mV s^{-1} or 100 mV s^{-1} in 0.5 m H_2SO_4. The potential window will depend on the activity of the catalysts, however, a potential window between -0.4 0.1 V vs. RHE for HER and 1.3-1.8 V for OER can be a good starting point. The dynamic degradation will be reported as % loss of activity after 1000-10000 HER/OER cycles. • The potential is set to the value at which the current density is 10 mA cm^{-2} (E_{10}). The steady-state degradation will be tested by the voltage decay determination after, at least 10-15 h of measurement.

5.2.3.3 Electrocatalyst testing in single cell

Single cell test in this report will be done with the cells the partners already have.

Testing Methods	Description
Single Cell Conditioning	• Single cell must be equilibrised at 80 °C with distilled water (<0.1 µS), fed to both compartments at ambient pressure, • A flow rate of 2 ml min^{-1} cm^{-2} will be maintained. • An applied load of 0.2 A cm^{-2} for 2 h (for *CRM catalysts*) or 0.05 A cm^{-2} (for *CRM-free catalysts*) for 24 hours to favour membrane hydration and in-situ purification. • This is only a guideline, and it can be adapted to reach the maximum performance
Polarization Curve	• Polarization curves are carried out in the galvanostatic mode by recording the cell voltage vs. the imposed current density. • For catalyst assessment in MEAs, the current density values are selected according to a logarithm mode between 0.005 and 2.2 V *(See Table 5 in Appendix*). • Allow the voltage to stabilise until a steady state conditions are achieved (± 2 mV/min). • If the steady state is not achieved in 2 mins change the step by sampling data and record the corresponding variation.

	• For a cell test at a fixed cell temperature, inlet temperature must be maintained at the same cell temperature. • The current density is preferably increased to the maximum achievable current with a cut-off voltage of 2.2 V. • At the end of the I-V curve measurements, the current density will be set to zero (OCV) before stopping all the testing equipment.

Influence of the cell temperature: By maintaining constant feed of the reactant as above, repeat the I-V curve measurements at increasing temperatures from RT or 30° to 90 °C (in steps of 10-20 °C). The cell temperature should be stabilised under OCV for a minimum of 20 minutes before proceeding with the next I-V curve measurement.

EIS	• EIS can be carried out in potentostatic or under galvanostatic mode. • EIS spectra of the anode can be recorded in potentiostatic mode starting from OCV thereafter at 1.5 V RHE, 1.8 V RHE; under galvanostatic mode at 50 mA cm^{-2} and maximum achieved current. • In the potentiostatic mode, apply a sinusoidal AC perturbation signal with an amplitude (peak-to-peak) of maximum 10 mV and a perturbation frequency in the 1 MHz to 10 mHz range as well as in the reverse order with 10 data points per decade in logarithmic spacing. • In the case of galvanostatic mode,10% sinusoidal oscillations. The impedance measurements are plotted as Nyquist plots (negative imaginary part vs. real part) and Bode plots (impedance amplitude, real and imaginary part vs. perturbation frequency and/or phase shift). • The cell ohmic resistance is determined from the series resistance i.e. from the high frequency intercept on the real axis. • The polarisation resistance is the difference between the low and the high frequency intercepts on the x-axis of the Nyquist plot.
Cyclic Voltammetry	• For ultra-low loading anodic CRM-based catalyst, this is carried out as specified for the half cell measurement by feeding humidified H_2 at the cathode (flow rate 100 ml min^{-1}). *Partners who do not have the cell capable of doing the test, will perform the test with existing single cells that they possess.* • The dew-point temperature is equal to cell temperature. • Reference cyclic voltammetry for the cathode is carried out as specified for the half cell measurement by feeding humidified H_2 at the anode (flow rate 100 ml min^{-1}). • The dew-point temperature is equal to cell temperature.

	• The Pt/H_2 interface acts both as reference (RHE) and counter electrode. Determination of the ECSA is reported above for the half cell.

This procedure can be in a first attempt adopted also with non-noble metal anode catalysts. Preferably, non-noble metal catalysts should be tested in half-cell with an external reference electrode. For anode characterization, since the oxygen evolution is the rate determining step, we assume that the anode contribution is prevailing, but the double layer capacitance contribution is lowered due to the contribution of both electrodes. Thus, the surface area determination from the capacitance values should be preferably carried out in half-cell.

Catalyst Stability	• For ultra-low loading CRM-based catalyst, steady-state galvanostatic cell operation at 1 or 2 A cm^{-2} for at least 1000 hrs is carried out under temperature and pressure relevant conditions. • Cell conditioning, water feed, selected cell hardware as above. • Data logging is at a frequency of 10^{-2} Hz. • Degradation rate in µV/h is estimated from the cell voltage raise vs. time using best fitting procedures. • Specific assessment of the dynamic behaviour for non CRM anode catalysts in single cell can be carried out by varying the anode potential between 1 and 1.8 V RHE (cell under electrolysis mode with reference electrode) and between 0 and -0.4 V vs. RHE for the cathode (hydrogen pumping mode). • These tests should be preferably of 1000 h with 1 min/step. Eventually, the single assessment of the electrodes dynamic behaviour can be replaced by the overall cell durability assessment for cycled operation (next point). • This test consist in 1000 hrs cycling between 1 – 1.8 V (vs RHE), 1 min/step, at relevant temperature and pressure operation conditions for a complete MEAs based on the selected anode and cathode catalysts (no in-situ reference electrode). • Under high cell potentials e.g. 1.8 V (vs RHE), the cathode, especially those based on non-CRM catalysts, will be negatively polarised vs. RHE as designed for the analysis of the dynamic behaviour in half-cell. Reference polarization curve and ac-impedance spectroscopy at the beginning and at the end of the experiment.

6 Data treatment: Determination of key performance indicators

Electrocatalyst performance evaluation in Half-cell & Single cell:

Initial experiments will be carried out in the presence of high catalyst loading (≤ 5 mg cm^{-2}) for CRM-free and ultra-low loadings (≤ 0.2 mg PGM Pt cm^{-2}) for precious catalysts.

Anode potential (E_a vs RHE) and overpotential ($E_a - E_{tn}$) will be measured from IR-free polarisation curves at 0.6 - 1 A cm^{-2} (CRM-free) and at 2 A cm^{-2} (reduced CRM) in liquid electrolyte or in MEAs under relevant temperature and pressure conditions.

A reference electrode is used in liquid electrolyte and values converted to RHE; Pt is used as cathode as reference/counter electrode in MEAs.

Cathode potential and overpotential (E_c vs RHE) measured at 1 (CRM-free) and 2 (reduced CRM) A cm^{-2} from the IR-free polarization curves carried out in liquid electrolytes in half cell or under hydrogen pumping mode in single cell.

A reference electrode is used in half-cell; in single cell a Pt reference electrode is used in the pumping mode. Alternatively, cathode potential is determined as the difference $E_c = E_{cell} - E_a$ where E_a is determined as above using a reference/counter Pt-based electrode. Catalyst loading ≤ 0.2 mg cm^{-2} for CRM-free and ≤ 0.05 mg PGM Pt cm^{-2} for ultra-low loadings precious catalysts.

Ohmic resistance for IR correction is determined from high frequency intercept on the real axis of the Nyquist plot obtained from AC-impedance spectroscopy and reported in Ohm cm^2.

For determining catalyst durability dynamic tests degradation reported as % in 1000 h (for cycling test 1-1.8 V vs. RHE, anode and 0 -0.4 V RHE cathode). For Steady-state degradation tests: voltage decay determined by curve fitting from galvanostatic durability test at 1-2 A cm^{-2}.

See Table 7 (in Appendix) for a sample sheet for characterization data.

7 Initial risk assessment

The CRMs reduction and the use of non-CRMs suppose risks that may occur with high probabilities and impacts and may affect performance, stability, and recycling of stack electrocatalysts and the objectives set out in the project. Regarding risk control, a risk identification and mitigation process (including qualitative and quantitative analysis) has been set among the Management Support Team (MST), supported by the WP Leaders. The process included and continues to include a plan of answers to develop options and actions, allowing reducing threats and increasing opportunities. Partners will be trained by DLR on the risk management to enhance the efficiency of risk approach all along project progress and in order to optimize continuously the answers to risks.
For catalyst development, the description of initial risk assessments is reported in the Table 4 along with the related probability occurrence and impact.
A mitigation process has been identified and proposed for each risk to meet the expectations set out in the project objectives with high probability and to facilitate margins for improvement.

Table 4 Baseline for risk assessments and mitigation actions

Description of risk	Probability	Impact	Proposed risk-mitigation measures
Bad performance, low efficiency, and stability of electrocatalysts	High	High	The best candidates will be selected considering as key priorities stack integration and results in single cells. This will enable the detection of any issue and of the required further improvement.
Poor possibilities for recycling of electrocatalysts compared to Life-cycle analysis goals (LCA)	Low	High	CRMs recycling and reduction strategies are a cornerstone to achieve the desired CAPEX reductions to approach energy storage markets. The previous experience from partners in the field will ensure progress in recycling of stack components as well as cost model and life cycle assessment respectively, supporting the components development towards circular economy considerations.
Performance of advanced catalysts is not as good as expected	Low	High	WP 1 aims at developing individual components including key steps such as materials selection, design and simulation tasks and development of a series of candidates for final selection to ensure that individual performance of the selected

			components will be best in class, meeting the expectations set out in the objectives with high probability.
CRM reduction for catalysts is lower than expected	Low	High	Most CRM reduction will be tackled by means of WP1, where the work will be oriented to develop and test at lab scale the performance of materials.

8 Reference

(1) Debe, M. K.; Hendricks, S. M.; Vernstrom, G. D.; Meyers, M.; Brostrom, M.; Stephens, M.; Chan, Q.; Willey, J.; Hamden, M.; Mittelsteadt, C. K.; Capuano, C. B.; Ayers, K. E.; Anderson, E. B. Initial Performance and Durability of Ultra-Low Loaded NSTF Electrodes for PEM Electrolyzers. *J. Electrochem. Soc.* **2012**, *159* (6), K165–K176. https://doi.org/10.1149/2.065206jes.

(2) Yu, H.; Danilovic, N.; Wang, Y.; Willis, W.; Poozhikunnath, A.; Bonville, L.; Capuano, C.; Ayers, K.; Maric, R. Nano-Size IrOx Catalyst of High Activity and Stability in PEM Water Electrolyzer with Ultra-Low Iridium Loading. *Appl. Catal. B Environ.* **2018**, *239*, 133–146. https://doi.org/10.1016/j.apcatb.2018.07.064.

(3) Siracusano, S.; Hodnik, N.; Jovanovic, P.; Ruiz-Zepeda, F.; Šala, M.; Baglio, V.; Aricò, A. S. New Insights into the Stability of a High Performance Nanostructured Catalyst for Sustainable Water Electrolysis. *Nano Energy* **2017**, *40*, 618–632. https://doi.org/10.1016/j.nanoen.2017.09.014.

(4) Lettenmeier, P.; Wang, L.; Golla-Schindler, U.; Gazdzicki, P.; Cañas, N. A.; Handl, M.; Hiesgen, R.; Hosseiny, S. S.; Gago, A. S.; Friedrich, K. A. Nanosized IrOx-Ir Catalyst with Relevant Activity for Anodes of Proton Exchange Membrane Electrolysis Produced by a Cost-Effective Procedure. *Angew. Chemie - Int. Ed.* **2016**, *55* (2), 742–746. https://doi.org/10.1002/anie.201507626.

(5) Wang, L.; Saveleva, V. A.; Zafeiratos, S.; Savinova, E. R.; Lettenmeier, P.; Gazdzicki, P.; Gago, A. S.; Friedrich, K. A. Highly Active Anode Electrocatalysts Derived from Electrochemical Leaching of Ru from Metallic Ir0.7Ru0.3 for Proton Exchange Membrane Electrolyzers. *Nano Energy* **2017**, *34*, 385–391. https://doi.org/10.1016/j.nanoen.2017.02.045.

(6) Lu, Z. X.; Shi, Y.; Gupta, P.; Min, X. ping; Tan, H. yi; Wang, Z. Da; Guo, C. qing; Zou, Z. qing; Yang, H.; Mukerjee, S.; Yan, C. F. Electrochemical Fabrication of IrOx Nanoarrays with Tunable Length and Morphology for Solid Polymer Electrolyte Water Electrolysis. *Electrochim. Acta* **2020**, *348*, 136302. https://doi.org/10.1016/j.electacta.2020.136302.

(7) Pham, C. Van; Bühler, M.; Knöppel, J.; Bierling, M.; Seeberger, D.; Escalera-López, D.; Mayrhofer, K. J. J.; Cherevko, S.; Thiele, S. IrO2 Coated TiO2 Core-Shell Microparticles Advance Performance of Low Loading Proton Exchange Membrane Water Electrolyzers. *Appl. Catal. B Environ.* **2020**, *269* (September 2019), 118762. https://doi.org/10.1016/j.apcatb.2020.118762.

(8) Rozain, C.; Mayousse, E.; Guillet, N.; Millet, P. Influence of Iridium Oxide Loadings on the Performance of PEM Water Electrolysis Cells: Part II - Advanced Oxygen Electrodes. *Appl. Catal. B Environ.* **2016**, *182*, 123–131. https://doi.org/10.1016/j.apcatb.2015.09.011.

(9) Wang, L.; Lettenmeier, P.; Golla-Schindler, U.; Gazdzicki, P.; Cañas, N. A.; Morawietz, T.; Hiesgen, R.; Hosseiny, S. S.; Gago, A. S.; Friedrich, K. A. Nanostructured Ir-Supported on Ti4O7 as a Cost-Effective Anode for Proton Exchange Membrane (PEM) Electrolyzers. *Phys. Chem. Chem. Phys.* **2016**, *18* (6), 4487–4495. https://doi.org/10.1039/c5cp05296c.

(10) Saveleva, V. A.; Wang, L.; Kasian, O.; Batuk, M.; Hadermann, J.; Gallet, J. J.; Bournel, F.; Alonso-Vante, N.; Ozouf, G.; Beauger, C.; Mayrhofer, K. J. J.; Cherevko, S.; Gago, A. S.; Friedrich, K. A.; Zafeiratos, S.; Savinova, E. R. Insight into the Mechanisms of High Activity and Stability of Iridium Supported on Antimony-Doped Tin Oxide Aerogel for Anodes of Proton Exchange Membrane Water Electrolyzers. *ACS Catal.* **2020**, *10* (4), 2508–2516. https://doi.org/10.1021/acscatal.9b04449.

(11) Böhm, D.; Beetz, M.; Schuster, M.; Peters, K.; Hufnagel, A. G.; Döblinger, M.; Böller, B.; Bein, T.; Fattakhova-Rohlfing, D. Efficient OER Catalyst with Low Ir Volume Density Obtained by Homogeneous Deposition of Iridium Oxide Nanoparticles on Macroporous Antimony-Doped Tin Oxide Support. *Adv. Funct. Mater.* **2020**, *30* (1). https://doi.org/10.1002/adfm.201906670.

(12) Gasteiger, H. A.; Kocha, S. S.; Sompalli, B.; Wagner, F. T. Activity Benchmarks and Requirements for Pt, Pt-Alloy, and Non-Pt Oxygen Reduction Catalysts for PEMFCs. *Appl. Catal. B Environ.*

2005, *56* (1-2 SPEC. ISS.), 9–35. https://doi.org/10.1016/j.apcatb.2004.06.021.

(13) Zheng, Y.; Jiao, Y.; Jaroniec, M.; Qiao, S. Z. Advancing the Electrochemistry of the Hydrogen-Evolution Reaction through Combining Experiment. *Angew. Chemie - Int. Ed.* **2015**, *54* (1), 52–65. https://doi.org/10.1002/anie.201407031.

(14) Shiva Kumar, S.; Himabindu, V. Hydrogen Production by PEM Water Electrolysis – A Review. *Mater. Sci. Energy Technol.* **2019**, *2* (3), 442–454. https://doi.org/10.1016/j.mset.2019.03.002.

(15) Ramli, Z. A. C.; Kamarudin, S. K. Platinum-Based Catalysts on Various Carbon Supports and Conducting Polymers for Direct Methanol Fuel Cell Applications: A Review. *Nanoscale Res. Lett.* **2018**, *13*. https://doi.org/10.1186/s11671-018-2799-4.

(16) Greeley, J.; Nørskov, J. K.; Kibler, L. A.; El-Aziz, A. M.; Kolb, D. M. Hydrogen Evolution over Bimetallic Systems: Understanding the Trends. *ChemPhysChem* **2006**, *7* (5), 1032–1035. https://doi.org/10.1002/cphc.200500663.

(17) Kitchin, J. R.; Nørskov, J. K.; Barteau, M. A.; Chen, J. G. Role of Strain and Ligand Effects in the Modification of the Electronic and Chemical Properties of Bimetallic Surfaces. *Phys. Rev. Lett.* **2004**, *93* (15), 4–7. https://doi.org/10.1103/PhysRevLett.93.156801.

(18) Wang, G.; Liu, J.; Sui, Y.; Wang, M.; Qiao, L.; Du, F.; Zou, B. Palladium Structure Engineering Induced by Electrochemical H Intercalation Boosts Hydrogen Evolution Catalysis. *J. Mater. Chem. A* **2019**, *7* (24), 14876–14881. https://doi.org/10.1039/c9ta03971f.

(19) European Commission. Commission of European Communities. Communication on the 2017 List of Critical Raw Materials for the EU (COM No. 490). **2017**, 1–8. https://doi.org/10.1017/CBO9781107415324.004.

(20) Yan, K. L.; Qin, J. F.; Lin, J. H.; Dong, B.; Chi, J. Q.; Liu, Z. Z.; Dai, F. N.; Chai, Y. M.; Liu, C. G. *Probing the Active Sites of Co3O4 for the Acidic Oxygen Evolution Reaction by Modulating the Co2+/Co3+ Ratio*; 2018; Vol. 6. https://doi.org/10.1039/c8ta00070k.

(21) Fenini, F.; Hansen, K. K.; Mogensen, M. B. Corrosion Study of Cr-Oxide Ceramics Using Rotating Ring Disk Electrode. **2019**, *166* (11). https://doi.org/10.1149/2.0191911jes.

(22) Hinnemann, B.; Moses, P. G.; Bonde, J.; Jørgensen, K. P.; Nielsen, J. H.; Horch, S.; Chorkendorff, I.; Nørskov, J. K. Ja0504690-1.Pdf. **2005**, 5308–5309. https://doi.org/10.1021/ja0504690.

(23) Jaramillo, T. F.; Jørgensen, K. P.; Bonde, J.; Nielsen, J. H.; Horch, S.; Chorkendorff, I. Identification of Active Edge Sites for Electrochemical H2 Evolution from MoS2 Nanocatalysts. *Science (80-.).* **2007**, *317* (5834), 100–102. https://doi.org/10.1126/science.1141483.

(24) Yan, Y.; Xia, B.; Xu, Z.; Wang, X. Recent Development of Molybdenum Sulfides as Advanced Electrocatalysts for Hydrogen Evolution Reaction. *ACS Catal.* **2014**, *4* (6), 1693–1705. https://doi.org/10.1021/cs500070x.

(25) Voiry, D.; Mohite, A.; Chhowalla, M. Phase Engineering of Transition Metal Dichalcogenides. *Chem. Soc. Rev.* **2015**, *44* (9), 2702–2712. https://doi.org/10.1039/c5cs00151j.

(26) Guo, Y.; Park, T.; Yi, J. W.; Henzie, J.; Kim, J.; Wang, Z.; Jiang, B.; Bando, Y.; Sugahara, Y.; Tang, J.; Yamauchi, Y. Nanoarchitectonics for Transition-Metal-Sulfide-Based Electrocatalysts for Water Splitting. *Adv. Mater.* **2019**, *31* (17), 1–34. https://doi.org/10.1002/adma.201807134.

(27) Meng, C.; Chen, X.; Gao, Y.; Zhao, Q.; Kong, D.; Lin, M.; Chen, X.; Li, Y.; Zhou, Y. Recent Modification Strategies of MoS2 for Enhanced Electrocatalytic Hydrogen Evolution. *Molecules* **2020**, *25* (5), 1–18. https://doi.org/10.3390/molecules25051136.

(28) Zhu, C.; Gao, D.; Ding, J.; Chao, D.; Wang, J. TMD-Based Highly Efficient Electrocatalysts Developed by Combined Computational and Experimental Approaches. *Chem. Soc. Rev.* **2018**, *47* (12), 4332–4356. https://doi.org/10.1039/c7cs00705a.

(29) Zhu, J.; Hu, L.; Zhao, P.; Lee, L. Y. S.; Wong, K. Y. Recent Advances in Electrocatalytic Hydrogen Evolution Using Nanoparticles. *Chem. Rev.* **2020**, *120* (2), 851–918. https://doi.org/10.1021/acs.chemrev.9b00248.

(30) Evolution, H. Iron Sulfide Materials : Catalysts for Electrochemical. *Inorganics* **2019**.

(31) Villalba, M.; Peron, J.; Giraud, M.; Tard, C. PH-Dependence on HER Electrocatalytic Activity of Iron Sulfide Pyrite Nanoparticles. *Electrochem. commun.* **2018**, *91* (April), 10–14. https://doi.org/10.1016/j.elecom.2018.04.019.
(32) Miao, R.; Dutta, B.; Sahoo, S.; He, J.; Zhong, W.; Cetegen, S. A.; Jiang, T.; Alpay, S. P.; Suib, S. L. Mesoporous Iron Sulfide for Highly Efficient Electrocatalytic Hydrogen Evolution. *J. Am. Chem. Soc.* **2017**, *139* (39), 13604–13607. https://doi.org/10.1021/jacs.7b07044.
(33) Jasion, D.; Barforoush, J. M.; Qiao, Q.; Zhu, Y.; Ren, S.; Leonard, K. C. Low-Dimensional Hyperthin FeS2 Nanostructures for Efficient and Stable Hydrogen Evolution Electrocatalysis. *ACS Catal.* **2015**, *5* (11), 6653–6657. https://doi.org/10.1021/acscatal.5b01637.
(34) Li, Z.; Xiao, M.; Zhou, Y.; Zhang, D.; Wang, H.; Liu, X.; Wang, D.; Wang, W. Pyrite FeS2/C Nanoparticles as an Efficient Bi-Functional Catalyst for Overall Water Splitting. *Dalt. Trans.* **2018**, *47* (42), 14917–14923. https://doi.org/10.1039/c8dt02927j.
(35) Chen, Y.; Xu, S.; Li, Y.; Jacob, R. J.; Kuang, Y.; Liu, B.; Wang, Y.; Pastel, G.; Salamanca-Riba, L. G.; Zachariah, M. R.; Hu, L. FeS2 Nanoparticles Embedded in Reduced Graphene Oxide toward Robust, High-Performance Electrocatalysts. *Adv. Energy Mater.* **2017**, *7* (19), 1–7. https://doi.org/10.1002/aenm.201700482.
(36) Jiang, J.; Zhu, L.; Chen, H.; Sun, Y.; Qian, W.; Lin, H.; Han, S. Highly Active and Stable Electrocatalysts of FeS2–Reduced Graphene Oxide for Hydrogen Evolution. *J. Mater. Sci.* **2019**, *54* (2), 1422–1433. https://doi.org/10.1007/s10853-018-2913-0.
(37) Guo, Y.; Shang, C.; Zhang, X.; Wang, E. Electrocatalytic Hydrogen Evolution Using the MS2@MoS2/RGO (M = Fe or Ni) Hybrid Catalyst. *Chem. Commun.* **2016**, *52* (79), 11795–11798. https://doi.org/10.1039/c6cc06180j.
(38) Ma, A.; Wang, C.; Lu, Y.; Wu, X.; Mamba, B. B.; Kuvarega, A. T.; Kefeni, K. K.; Gui, J.; Liu, D. Ultrathin NiFeS Nanomeshes with Sulfur Vacancy for Electrocatalytic Hydrogen Evolution. *ChemElectroChem* **2020**, *7* (9), 2199–2204. https://doi.org/10.1002/celc.202000477.
(39) Zhao, C.; Zhang, C.; Bhoyate, S.; Kahol, P. K.; Kostoglou, N.; Mitterer, C.; Hinder, S.; Baker, M.; Constantinides, G.; Polychronopoulou, K.; Rebholz, C.; Gupta, R. K. Nanostructured Fe-Ni Sulfide: A Multifunctional Material for Energy Generation and Storage. *Catalysts* **2019**, *9* (7). https://doi.org/10.3390/catal9070597.
(40) Cao, D.; Kang, W.; Huang, Z.; Li, H.; Yang, M.; Li, J.; Gao, Y.; Wang, Y.; Ma, P.; Sun, D. N-Doped Carbon Matrix Supported Fe3Ni6S8 Hierarchical Architecture with Excellent Sodium Storage Capability and Electrocatalytic Properties. *Electrochim. Acta* **2019**, *325*, 134925. https://doi.org/10.1016/j.electacta.2019.134925.
(41) Liu, C.; Guo, Y.; Yu, Z.; Wang, H.; Yao, H.; Li, J.; Shi, K.; Ma, S. Hierarchical Microsphere Assembled by Nanoplates Embedded with MoS2 and (NiFe)S x Nanoparticles as Low-Cost Electrocatalyst for Hydrogen Evolution Reaction. *Nanotechnology* **2020**, *31* (3). https://doi.org/10.1088/1361-6528/ab485d.
(42) Jiang, J.; Zhu, L.; Chen, H.; Sun, Y.; Lin, H.; Han, S. Effect of Nickel-Doped FeS2 Nanoparticles-Reduced Graphene Oxide Electrocatalysts for Efficient Hydrogen Evolution. *J. Alloys Compd.* **2019**, *775*, 1293–1300. https://doi.org/10.1016/j.jallcom.2018.10.261.
(43) Yan, S.; Wang, K.; Zhou, F.; Lin, S.; Song, H.; Shi, Y.; Yao, J. Ultrafine Co:FeS2/CoS2 Heterostructure Nanowires for Highly Efficient Hydrogen Evolution Reaction. *ACS Appl. Energy Mater.* **2020**, *3* (1), 514–520. https://doi.org/10.1021/acsaem.9b01769.
(44) Huang, S.-Y.; Sodano, D.; Leonard, T.; Luiso, S.; Fedkiw, P. S. Cobalt-Doped Iron Sulfide as an Electrocatalyst for Hydrogen Evolution. *J. Electrochem. Soc.* **2017**, *164* (4), F276–F282. https://doi.org/10.1149/2.0761704jes.
(45) Huang, G.; Xu, S.; Liu, Z.; Yuan, S.; Zhang, C.; Ai, J.; Li, N.; Li, X. Ultrafine Cobalt-Doped Iron Disulfide Nanoparticles in Ordered Mesoporous Carbon for Efficient Hydrogen Evolution. *ChemCatChem* **2020**, *12* (3), 788–794. https://doi.org/10.1002/cctc.201901759.

(46) Amstutz, V.; Toghill, K. E.; Powlesland, F.; Vrubel, H.; Comninellis, C.; Hu, X.; Girault, H. H. Renewable Hydrogen Generation from a Dual-Circuit Redox Flow Battery. *Energy Environ. Sci.* **2014**, *7* (7), 2350–2358. https://doi.org/10.1039/c4ee00098f.
(47) Mills, A.; Mcmurray, N. + 0,. (1). **1989**, *85* (8), 2055–2070.
(48) Reed, K.; Cormack, A.; Kulkarni, A.; Mayton, M.; Sayle, D.; Klaessig, F.; Stadler, B. Exploring the Properties and Applications of Nanoceria: Is There Still Plenty of Room at the Bottom? *Environ. Sci. Nano* **2014**, *1* (5), 390–405. https://doi.org/10.1039/c4en00079j.
(49) Arenas, L. F.; Ponce De León, C.; Walsh, F. C. Electrochemical Redox Processes Involving Soluble Cerium Species. *Electrochim. Acta* **2016**, *205*, 226–247. https://doi.org/10.1016/j.electacta.2016.04.062.
(50) Posternak, M.; Baldereschi, A.; Delley, B. Dissociation of Water on Anatase TiO2 Nanoparticles: The Role of Undercoordinated Ti Atoms at Edges. *J. Phys. Chem. C* **2009**, *113* (36), 15862–15867. https://doi.org/10.1021/jp9032113.
(51) Banfield, J. F.; Zhang, H. Thermodynamic Analysis of Phase Stability of Nanocrystalline Titania. *J. Mater. Chem.* **1998**, *8* (9), 2073–2076.
(52) Abadias, G.; Gago, A. S.; Alonso-Vante, N. Structural and Photoelectrochemical Properties of Ti1-XWxO2 Thin Films Deposited by Magnetron Sputtering. *Surf. Coatings Technol.* **2011**, *205* (SUPPL. 2), S265–S270. https://doi.org/10.1016/j.surfcoat.2011.02.011.
(53) Chae, S. Y.; Park, M. K.; Lee, S. K.; Kim, T. Y.; Kim, S. K.; Lee, W. I. Preparation of Size-Controlled TiO2 Nanoparticles and Derivation of Optically Transparent Photocatalytic Films. *Chem. Mater.* **2003**, *15* (17), 3326–3331. https://doi.org/10.1021/cm030171d.
(54) Nong, H. N.; Gan, L.; Willinger, E.; Teschner, D.; Strasser, P. IrOx Core-Shell Nanocatalysts for Cost- and Energy-Efficient Electrochemical Water Splitting. *Chem. Sci.* **2014**, *5* (8), 2955–2963. https://doi.org/10.1039/c4sc01065e.
(55) Lee, Y.; Suntivich, J.; May, K. J.; Perry, E. E.; Shao-Horn, Y. Synthesis and Activities of Rutile IrO 2 and RuO 2 Nanoparticles for Oxygen Evolution in Acid and Alkaline Solutions. *J. Phys. Chem. Lett.* **2012**, *3* (3), 399–404. https://doi.org/10.1021/jz2016507.
(56) Retuerto, M.; Pascual, L.; Calle-Vallejo, F.; Ferrer, P.; Gianolio, D.; Pereira, A. G.; García, Á.; Torrero, J.; Fernández-Díaz, M. T.; Bencok, P.; Peña, M. A.; Fierro, J. L. G.; Rojas, S. Na-Doped Ruthenium Perovskite Electrocatalysts with Improved Oxygen Evolution Activity and Durability in Acidic Media. *Nat. Commun.* **2019**, *10* (1). https://doi.org/10.1038/s41467-019-09791-w.
(57) Ji, H.; Liu, D.; Cheng, H.; Yang, L.; Zhang, C.; Zheng, W. Facile Synthesis and Electrical Switching Properties of V2O3 Powders. *Mater. Sci. Eng. B Solid-State Mater. Adv. Technol.* **2017**, *217*, 1–6. https://doi.org/10.1016/j.mseb.2017.01.003.
(58) Kysar, J.; Sekhar, P. K. Facile Synthesis of Vanadium Oxide Nanowires. *Appl. Nanosci.* **2016**, *6* (7), 959–964. https://doi.org/10.1007/s13204-015-0508-5.
(59) Liao, L.; Wang, S.; Xiao, J.; Bian, X.; Zhang, Y.; Scanlon, M. D.; Hu, X.; Tang, Y.; Liu, B.; Girault, H. H. A Nanoporous Molybdenum Carbide Nanowire as an Electrocatalyst for Hydrogen Evolution Reaction. *Energy Environ. Sci.* **2014**, *7* (1), 387–392. https://doi.org/10.1039/c3ee42441c.
(60) Gao, Q.; Zhang, C.; Xie, S.; Hua, W.; Zhang, Y.; Ren, N.; Xu, H.; Tang, Y. Synthesis of Nanoporous Molybdenum Carbide Nanowires Based on Organic - Inorganic Hybrid Nanocomposites with Sub-Nanometer Periodic Structures. *Chem. Mater.* **2009**, *21* (23), 5560–5562. https://doi.org/10.1021/cm9014578.
(61) Naga Mahesh, K.; Balaji, R.; Dhathathreyan, K. S. Palladium Nanoparticles as Hydrogen Evolution Reaction (HER) Electrocatalyst in Electrochemical Methanol Reformer. *Int. J. Hydrogen Energy* **2016**, *41* (1), 46–51. https://doi.org/10.1016/j.ijhydene.2015.09.110.
(62) Laursen, A. B.; Patraju, K. R.; Whitaker, M. J.; Retuerto, M.; Sarkar, T.; Yao, N.; Ramanujachary, K. V.; Greenblatt, M.; Dismukes, G. C. Nanocrystalline Ni5P4: A Hydrogen Evolution Electrocatalyst of Exceptional Efficiency in Both Alkaline and Acidic Media. *Energy Environ. Sci.* **2015**, *8* (3),

1027–1034. https://doi.org/10.1039/c4ee02940b.

(63) Popczun, E. J.; McKone, J. R.; Read, C. G.; Biacchi, A. J.; Wiltrout, A. M.; Lewis, N. S.; Schaak, R. E. Nanostructured Nickel Phosphide as an Electrocatalyst for the Hydrogen Evolution Reaction. *J. Am. Chem. Soc.* **2013**, *135* (25), 9267–9270. https://doi.org/10.1021/ja403440e.

(64) Popczun, E. J.; Roske, C. W.; Read, C. G.; Crompton, J. C.; McEnaney, J. M.; Callejas, J. F.; Lewis, N. S.; Schaak, R. E. Highly Branched Cobalt Phosphide Nanostructures for Hydrogen-Evolution Electrocatalysis. *J. Mater. Chem. A* **2015**, *3* (10), 5420–5425. https://doi.org/10.1039/c4ta06642a.

(65) McEnaney, J. M.; Chance Crompton, J.; Callejas, J. F.; Popczun, E. J.; Biacchi, A. J.; Lewis, N. S.; Schaak, R. E. Amorphous Molybdenum Phosphide Nanoparticles for Electrocatalytic Hydrogen Evolution. *Chem. Mater.* **2014**, *26* (16), 4826–4831. https://doi.org/10.1021/cm502035s.

(66) McEnaney, J. M.; Chance Crompton, J.; Callejas, J. F.; Popczun, E. J.; Read, C. G.; Lewis, N. S.; Schaak, R. E. Electrocatalytic Hydrogen Evolution Using Amorphous Tungsten Phosphide Nanoparticles. *Chem. Commun.* **2014**, *50* (75), 11026–11028. https://doi.org/10.1039/c4cc04709e.

(67) Callejas, J. F.; McEnaney, J. M.; Read, C. G.; Crompton, J. C.; Biacchi, A. J.; Popczun, E. J.; Gordon, T. R.; Lewis, N. S.; Schaak, R. E. Electrocatalytic and Photocatalytic Hydrogen Production from Acidic and Neutral-PH Aqueous Solutions Using Iron Phosphide Nanoparticles. *ACS Nano* **2014**, *8* (11), 11101–11107. https://doi.org/10.1021/nn5048553.

(68) Pan, Y.; Liu, Y.; Zhao, J.; Yang, K.; Liang, J.; Liu, D.; Hu, W.; Liu, D.; Liu, Y.; Liu, C. Monodispersed Nickel Phosphide Nanocrystals with Different Phases: Synthesis, Characterization and Electrocatalytic Properties for Hydrogen Evolution. *J. Mater. Chem. A* **2015**, *3* (4), 1656–1665. https://doi.org/10.1039/c4ta04867a.

(69) Farsadrooh, M.; Torrero, J.; Pascual, L.; Peña, M. A.; Retuerto, M.; Rojas, S. Two-Dimensional Pd-Nanosheets as Efficient Electrocatalysts for Ethanol Electrooxidation. Evidences of the C–C Scission at Low Potentials. *Appl. Catal. B Environ.* **2018**, *237*, 866–875. https://doi.org/10.1016/j.apcatb.2018.06.051.

(70) Lettenmeier, P.; Majchel, J.; Wang, L.; Saveleva, V. A.; Zafeiratos, S.; Savinova, E. R.; Gallet, J. J.; Bournel, F.; Gago, A. S.; Friedrich, K. A. Highly Active Nano-Sized Iridium Catalysts: Synthesis and Operando Spectroscopy in a Proton Exchange Membrane Electrolyzer. *Chem. Sci.* **2018**, *9* (14), 3570–3579. https://doi.org/10.1039/c8sc00555a.

(71) European Commission (EC). Critical Raw Materials Resilience: Charting a Path towards Greater Security and Sustainability. **2020**, (COM no. 474, 2020).

Acknowledgement

This project has received funding from the European Union's Horizon 2020 research and innovation programme under grant agreement No 862253".

Appendix

Table 5 Protocols for polarization curves in half-cell and Single cell

Current Density ($A \cdot cm^{-2}$)	Cell Voltage (V)
0.0005	
0.001	
0.002	
0.005	
0.01	
0.02	
0.03	
0.04	
0.06	
0.08	
0.1	
0.15	
0.2	
0.25	
0.3	
0.35	
0.4	

Current Density ($A \cdot cm^{-2}$)	Cell Voltage (V)
0.45	
0.5	
0.6	
0.7	
0.8	
0.9	
1	
1.1	
1.2	
1.3	
1.4	
1.5	
1.6	
1.7	
1.8	
1.9	
2	

Table 6 KPIs in RDE testing

Indicators	Fresh Catalyst	Used catalysts after 10000 cycles
E_{onset} @ 1 mA cm^{-2}		
E_{10} @ 10 mA cm^{-2}		
E_{100} @ 100 mA cm^{-2}		
Tafel plots		
j_0		

Table 7 Table of Characterization Data

	unit	result	method
Catalyst/support formulation			
Batch No			
Application as anode or cathode			
Bulk and possibly surface composition			
Physico-chemical parameters: structure			
Physico-chemical parameters: particle size/crystallite size	nm		
Electrochemically active surface area	m^2/g; mC/mg $mC\ cm^{-2}$ $mF\ mg^{-1}$ $mF\ cm^{-2}$		
IR-free anode potential (E_a vs RHE) *and over-potential* ($E_a - E_{tn}$) measured at 0.6 - 1 A cm^{-2} (CRM-free) and at 2 A cm^{-2} (reduced CRM). Data reported at specific loading (mg cm^{-2}) in the presence of specific electrolyte, temperature (°C) and pressure (bar) conditions	V vs RHE V vs E_{tn}		
cathode potential and overpotential (Ec vs RHE) measured at 1 and 2 A cm-2 at specific loading (mg cm^{-2}) in the presence of specific electrolyte, temperature (°C) and pressure (bar) conditions	V vs RHE		
Steady-state Durability: Voltage loss in 1000 h steady state tests at 1 or 2 A cm^{-2}	µV/h		
Dynamic Performance Degradation in MEAs in 1000 h dynamic tests (cell 1-1.8 V, 1 min/step)	%		
Dynamic Performance Degradation in half cell in a 1000 h dynamic tests (anode 1-1.8 V RHE, cathode 0—0.4 V RHE, 1 min/step)	%		
Electrochemical surface area loss in accelerated tests vs. initial conditions	%		